Delft University of Technology

MMC Control in HVDC System connected to Offshore wind farms

Control Strategy for asymmetric offshore AC faults

Cherat, Naajein - 5857228

MMC Control in HVDC System connected to Offshore wind farms

Control Strategy for asymmetric offshore AC faults

by

Naajein Cherat

to obtain the degree of Master of Science in Sustainable Energy Technology

at the Delft University of Technology,

to be defended publicly on Tuesday July 9, 2024 at 13:30 PM.

Student number:	5857228	
Project duration:	November 13, 2023 – July 9, 2024	
Thesis committee:	Prof. Dr. P. Palensky,	EWI-ESE-IEPG, TU Delft,
	Dr. A. Lekic,	EWI-ESE-IEPG, TU Delft
	Dr. H. Vahedi	EWI-ESE-DCE&S, TU Delft
	Dr. V. Nougain,	EWI-ESE-IEPG, TU Delft

This thesis is confidential and cannot be made public until December 31, 2024.

Cover: Alpha Ventus Windmills / SteKrueBe / Wikimedia / CC BY-SA 3.0
Style: TU Delft Report Style, with modifications by Daan Zwaneveld

An electronic version of this thesis is available at http://repository.tudelft.nl/.

TU Delft

Preface

The master thesis titled **"MMC Control in HVDC System Connected to Offshore Wind Farms"** is written to fulfill the graduation requirements of the MSc. Sustainable Energy Technology program at Delft University of Technology. The motivation for this thesis stems from the ongoing shift from conventional power generation units to power converter-interfaced generation units. Offshore wind farms are rapidly expanding as a renewable energy source. Modular multilevel converters (MMCs) enhance High Voltage Direct Current (HVDC) systems with features like modularity, reliability, and effective fault handling, making them cost-effective for offshore wind farm integration. One of the critical contingency affecting the stability of MMC-based HVDC systems is the short circuit faults, highlighting the need for effective fault ride-through strategies, particularly for offshore AC faults, which are often neglected in research.

I have a strong passion for the energy transition, particularly in renewable energy integration. To prepare for this thesis, I conducted a literature review on topics related to the control actions for integrating offshore wind farms into the grid. Since MMC was a new concept for me, I spent the initial months learning more about the converters and then focused on converter control strategies, given my limited background in control systems. During my literature research, I became intrigued by the system behavior due to offshore asymmetrical faults. I also spent a considerable amount of time understanding the Real Time Digital Simulator (RTDS) environment for modeling power systems in real-time.

This thesis could not have been completed without the help of many people. Firstly, I would like to extend my heartfelt gratitude to my supervisors, Dr. Aleksandra Lekić and Prof. Dr. Peter Palensky. I am especially grateful to Dr. Lekić for introducing me to the topic of MMC control. Her guidance and encouragement have been invaluable. Immense appreciation goes to my daily supervisor, Dr. Vaibhav Nougain, for clarifying all my queries patiently and offering words of encouragement throughout the duration of the thesis. His constant guidance helped me in finalizing my focus areas for this thesis. I would also like to thank Remko Koorneef for helping me install the RTDS software and for being patient whenever I encountered issues. Special mentions go to Pieter Gommers, Ajay Shetgaonkar, and Rohan K Tarcar for lending a helping hand in clearing my doubts. Furthermore, I would like to thank Dr. Hani Vahedi for agreeing to be part of the thesis committee and evaluating my work and report.

Lastly, I would like to express my deep gratitude to my friends and family for their support.

Naajein Cherat
Delft, July 2024

Summary

Modular Multilevel Converter (MMC) based High Voltage Direct Current (HVDC) system is considered as a cost effective option for the integration of offshore wind farms. One of the critical contingency affecting the stability of MMC-HVDC system is the short circuit faults. Effective fault ride through (FRT) strategies are essential to prevent the disconnection of HVDC converter station from the AC grid. FRT capability studies for MMC-HVDC systems have traditionally focused on onshore AC grid faults and DC link faults. Offshore AC faults, particularly asymmetrical faults, have not received significant attention in the literature. This thesis proposes an event-triggered control strategy to stabilize the system once the offshore AC fault has occurred, identified, and isolated. The strategy employs different types of control actions such as the widely-used proportional-integral (PI) controller and the advanced super-twisted sliding mode controller (STSMC) to smoothly transition the post-fault system to a new steady state operating point by suppressing the negative sequence current.

Sequence component analysis is used to break down the system's behavior during faults into positive sequence, negative sequence, and zero sequence components. This approach enables a comprehensive understanding of fault conditions and their effects on system stability. When a fault occurs, a sudden increase in negative sequence current activates the proposed control strategy. This control strategy remains active for a specified duration before reverting to original control settings once the system stabilizes. The duration of the control strategy's implementation depends on the fault type (Line-Ground, Line-Line, or Line-Line-Ground), with more severe faults requiring longer stabilization periods. Consequently, it is essential to classify faults. Sequence components are utilized to detect faults and classify different types of asymmetrical faults.

Initially, the thesis explores the impact of a negative sequence current control scheme on the transient behavior of the power system using a PI controller. The PI controller, known for its simplicity and robustness, is widely used in MMC control. However, its performance may be compromised under uncertain disturbances, such as those introduced by asymmetrical faults. To address the limitations of the PI controller, the thesis proposes a non-linear control strategy using STSMC. The STSMC offers several advantages, including faster convergence and enhanced robustness to system uncertainties and parameter variations. By employing STSMC, the system can achieve quicker stabilization post-fault compared to the PI control action.

The proposed control operations are designed to be event-triggered, meaning they are activated only in the presence of a fault. This approach ensures that the control strategy is dynamically responsive, engaging only when necessary to address fault conditions. The validity of the proposed strategy is demonstrated through simulations on a ±525 kV, three-terminal meshed MMC-HVDC system model using Real-Time Digital Simulator (RTDS). The simulations illustrate the effectiveness of the event-triggered control in stabilizing the system post-fault, highlighting the superior performance of the STSMC compared to the traditional PI controller. This study addresses a critical gap in the literature by focusing on the stabilization of MMC-HVDC systems under offshore AC faults, particularly asymmetrical faults. The proposed event-triggered control strategy offers an effective solution to enhance the fault ride-through capability and ensure the reliable integration of offshore wind power plants into the grid.

Contents

List of Figures

List of Tables

1 Introduction

This chapter introduces the problem statement and explains the motivation for selecting this specific problem. It also outlines a set of research questions identified to guide the work throughout the thesis.

1.1. Motivation

Offshore wind farms are experiencing rapid growth as a sustainable energy solution, attributed to their advantages of reduced wind variability and space constraints [1]. High voltage direct current (HVDC) is a proven technology for the grid integration of offshore wind farms. HVDC grid is used in power transmissions networks due to its high-power transmission capacity over long distances. Modular multilevel converters (MMC) are used in HVDC transmission systems due to their distinctive features such as modular structure, high reliability, effective redundancy, simple fault identification, and clearance [2]. Owing to its grid-forming ability and control capability, the MMC-HVDC-based power system is considered a cost-effective option for the integration of offshore wind farms [3].

One of the critical contingencies affecting the stability of MMC-based HVDC systems is the short circuit fault [4]. This can result in power system instability. An effective fault ride-through strategy is critical to avoid HVDC converter station disconnection from the AC grid. The literature for research on short-circuit faults in HVDC systems has primarily focused on the DC link and onshore AC grid faults [5], neglecting the offshore AC fault contingency. In conventional onshore power systems, the presence of synchronous generators offer high short circuit current (positive sequence in case of symmetrical faults and negative in case of asymmetrical fault) which allow the protection system to detect and clear the fault securely [2]. For a network without synchronous generators, such as offshore ac network of HVDC connected wind power plants, the fault ride through strategy is not fine-tuned to ensure the secure operation of protection.

Asymmetrical AC faults (single-phase-to-ground, phase-to-phase, and phase-to-phase-to-ground) represent the most probable fault contingencies in the AC power system [6]. On the occurrence of an asymmetrical fault, large negative sequence currents will be generated in the system. Due to the over-current limitations imposed by the converters, the control strategy of negative sequence current under asymmetric AC faults is of great significance [6]. Understanding offshore AC grid fault behaviors, particularly concerning the characterization of negative sequence current, is pivotal for protection mechanisms.

1.2. Problem Definition

In the event of an unbalanced faults, conventional generation units typically act as voltage sources in the positive sequence circuit, leading to high fault currents. However, power converter-interfaced generation units behave differently. They function as controlled current sources in both the positive and negative sequence circuits, while the zero sequence circuit remains mostly open due to transformer configuration [7]. Suppressing negative sequence current is a common strategy during unbalanced voltage conditions to protect the switching valves from uncontrolled fault currents. However, this can lead to increased risk of mal-operation due to absence of fault currents which can also prevent the recovery of ac voltage post fault [8].

The impact of negative sequence current control schemes on an onshore AC transmission line during an unbalanced onshore grid fault is analyzed in [7]. Two scenarios are considered, the suppression of negative sequence current and injection of negative sequence current proportionally to the negative sequence voltage. It is shown that injecting negative sequence current enhances fault detection capabilities and improves the performance of protection schemes in comparison to suppression of negative sequence current.

A control strategy that utilizes negative sequence voltages to facilitate controlled injection of negative sequence currents during offshore asymmetric AC faults is proposed in [8]. It is shown that by actively managing negative sequence currents and voltages, the strategy ensures a controlled level of fault current and prevents overvoltage conditions in healthy phases post-fault. This approach not only enhances the stability and reliability of the offshore wind power transmission system but also minimizes the risk of protection mal-operation. An enhancement to the control strategy proposed in [8] is done in [3]. The per unit value of the MMC valve-side voltage positive sequence component is used as the droop coefficient, aiming to reduce over-adjustment issues in AC voltage during fault periods. The over-adjustment of AC voltage can lead to a significant reduction in the active power transmission of the HVDC system in case of a large voltage drop.

A high-performance fault ride-through method for an MMC-integrated offshore wind farm system, showcasing responses to symmetric and asymmetric faults is presented in [9]. A method for continuous power transmission under faults and effective suppression of overcurrent is proposed to achieve FRT in [9].Negative sequence current control strategy for severe asymmetric offshore AC faults is discussed in [6]. The strategy in [6] aims to address the issue of transient overcurrent by coordinating the control of the negative sequence current in the GSC (grid-side converters) of the wind plant and the offshore MMC. When there is a severe asymmetric AC fault, the control strategy ensures that the negative sequence current of the offshore MMC is suppressed to zero, while the GSC cooperates to reduce the positive sequence current. The strategy involves limiting the positive sequence current of the GSC and reducing the positive sequence voltage of the offshore MMC to reserve margins for the modulation of the negative sequence voltage.

Different control strategies, ranging from classical to advanced, have been developed to control MMCs and regulate the current and power of MMCs. The widely used Proportional Integral (PI) and Proportional Resonant (PR) controllers are common choices for MMC control due to its simplicity and robustness. However, during uncertain disturbances in the power system, the performance of these controllers may decline [10]. Furthermore, the nonlinear characteristics of MMCs have emphasized the necessity of exploring nonlinear controllers to improve system performance. The different non-linear controllers investigated in the literature are Model Predictive Control (MPC), Back-Stepping Control (BSC) and Sliding Mode Control (SMC). MPC's offer numerous advantages such as their capability for multiple input multiple output (MIMO) control and their robust and fast response, making them a favoured option in power electronics applications [11]. However, MPC suffer from high computational burden and the necessity for an accurate model of the MMC's [12].

The BSC approach offers a systematic method for designing a control system that tracks a desired reference signal by choosing an appropriate Lyapunov function. It is designed by recursively treating certain state variables as virtual controls and formulating intermediate control laws. However, BSC is sensitive to parameter uncertainties [13]. The adoption of SMC in power converters have gained significant interest lately, mainly due to its fast response, robustness to uncertainties, resilience to parameter variations and ease of implementation. However, the discontinuous nature of control signal leads to chattering effects [10]. One approach to reduce the chattering effect is to use second-order sliding mode control which converts discontinuous function to a continuous function such as the super twisting sliding mode control (STSMC) [12].

This study focuses on an event-triggered suppression of negative sequence current to improve the overall transient behavior of the power system during an unbalanced offshore grid fault, aiming to restore system stability post-fault clearance. Linear (PI) and non-linear (STSMC) controllers are tested for their effectiveness in restoring the system. Since non-linear controllers have a faster convergence compared to their linear PI counterparts, the proposed non-linear controller is well suited to counter the non-linear dynamics of MMC converters. The proposed control strategy is tested on a $\pm$525 kV three-terminal meshed MMC-HVDC system modeled in Real Time Digital Simulator (RTDS).

1.3. Research Questions

To guide the work for this thesis, the following research questions have been identified and will be addressed:

1. What are the potential issues during an asymmetrical fault?
2. What are the characteristics of sequence components during unbalanced fault?
3. How can the sequence current control be utilized to enhance the transient behavior of offshore wind power plants connected to MMC-HVDC systems during unbalanced faults?
4. How does the dynamic response of the power system improve with the implementation of non-linear control for the MMC converter compared to classical PI control?

1.4. Thesis Outline

This report is divided into 7 main chapters. Chapter 1 gives an outline of the motivation and problem statement of the thesis. In Chapter 2, basic structure of MMC and its general controls are explained. The power system fault analysis and sequence component characteristics of the system during ac faults are dealt in Chapter 3. Description of the three terminal meshed MMC-HVDC transmission system and the various converter controls used are covered in Chapter 4. Chapter 5 outlines the linear and non linear control algorithms used in the study. Relevant results proving the validity of the proposed controller are presented in Chapter 6. Lastly, Chapter 7 presents the conclusions derived from the study as well as suggestions for further research.

2
Modular Multilevel Converter (MMC)

This chapter presents the basic structure and mathematical model of MMC. The control algorithms as well the main control strategies for MMC are also included in this chapter.

2.1. Basic structure of MMC

With the advancement of high-power semiconductors, particularly controllable switches, the HVDC technology has undergone significant evolution. This progression has transitioned from Line Commutated Converters (LCC), based on thyristor technology, to Voltage Source Converter (VSC) technology, which utilizes Insulated-Gate Bipolar Transistors (IGBTs). More recently, VSC technology has further advanced, moving from traditional two and three-level systems to Multi-Level Modular Converter (MMC) systems [14]. MMC is considered the most favorable converter topology when compared to other VSC configurations due to its advantages such as enhanced modularity and controllability, increased efficiency, and a reduced converter footprint [15]. Additional benefits of the MMC include minimized switching losses and the elimination of extra filtering requirements, as it generates negligible high-frequency harmonics due to its precise sinusoidal approximation.

Basic structure of a three-phase MMC is given in Figure 2.1 [11]. Each phase is denoted by a leg and each leg consists of two arms - the upper and lower arm. Both the arms comprise N series connected identical sub modules (SM). Each arm has a series inductor and resistance. Inductor is used to limit the high frequency components in the arm currents. SMs are inserted or bypassed to generate the desired phase voltages. MMC control provide the signals indicating which SM to be inserted or bypassed.

Out of the different configurations of SMs, half bridge(HB) circuit is the most popular one as only two switches are used, resulting in smaller switching losses and less complexity. As shown in Figure 2.1, HB SM has two switches and one capacitor. By controlling the switches, the output of SM has three states. When S1 is on and S2 is off, the output voltage is equal to capacitor voltage which is called the on-state or inserted state. When S1 is off and S2 is on, output voltage is 0 which is called bypassed state. When both switches are off, SM is blocked which happens during a fault to avoid capacitor short circuit. The direction of arm current also affect the output voltage. When SM is inserted, and current is positive it means capacitor is charged and if current is negative, capacitor is discharged. Different states of sub modules are given in Table 2.1 and graphically represented in Figure 2.2 [16].

2.2. Mathematical model of MMC

Figure 2.1 is used to derive dynamic equation for MMC. The voltage of the inserted sub modules on each arm are given as $v_{j,k}$ where j represents the arms on each leg (upper (u) and lower (l)) and k represents the phase (a, b, c). The arm voltages $v_{j,k}$ can be calculated by the Equation 2.1 assuming all the capacitors within the arm are equally balanced.

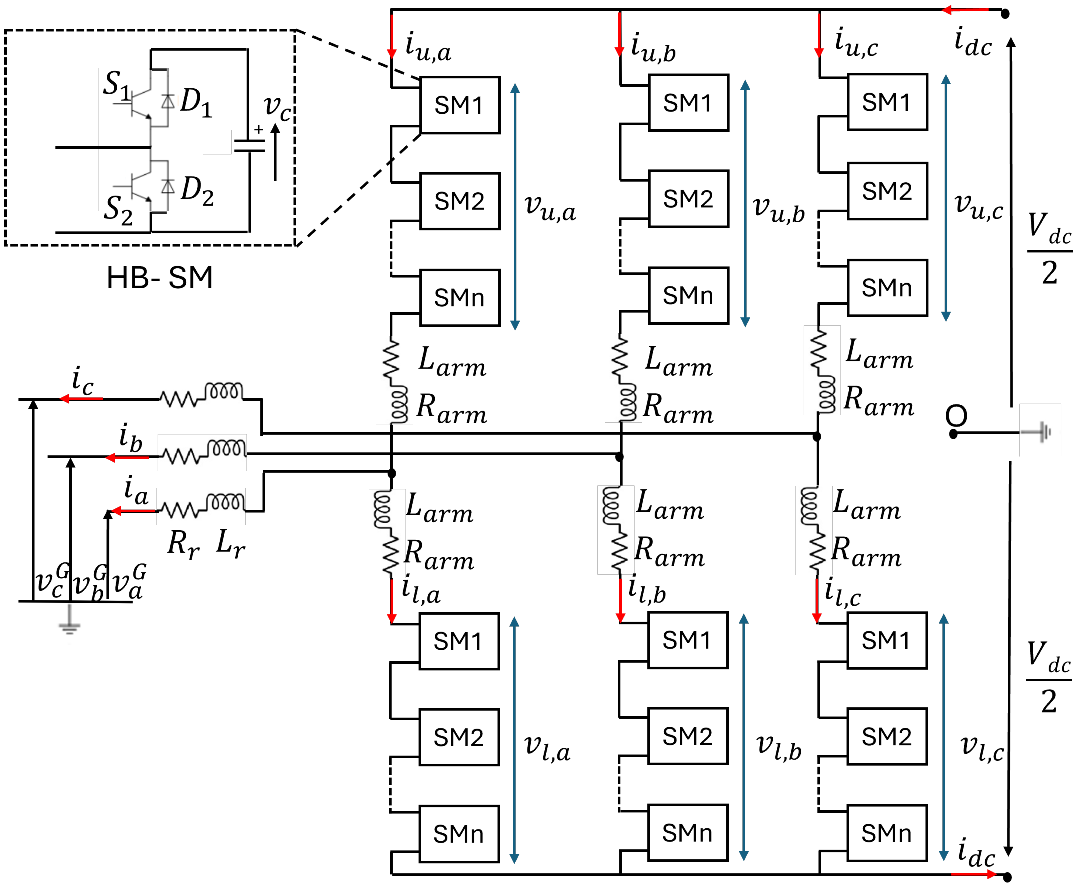

Figure 2.1: Structure of MMC

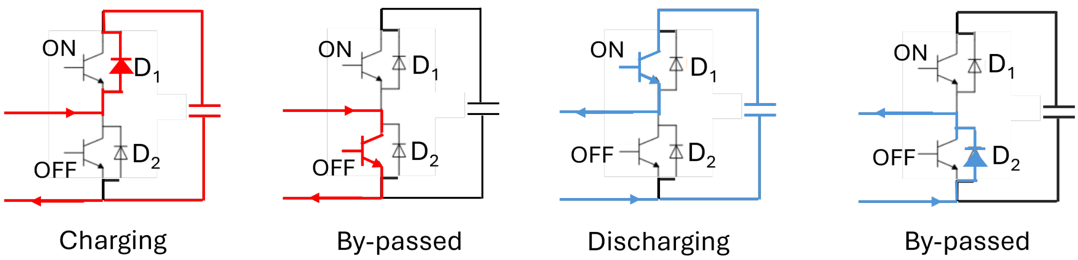

Figure 2.2: State of SM capacitor

$$v_{j,k} = n_{j,k} v_{cj,k} \tag{2.1}$$

where, $v_{cj,k}$ is the capacitor voltages of individual SMs and $n_{j,k}$ is the number of SMs inserted in lower and upper arms.

Due to the symmetry between upper and lower arm, the AC side current i_k will be equally divided into two parts flowing to upper and lower arm respectively. The DC current i_{dc} is also split equally into three parts for three phases due to the symmetry between the three phases [16]. Thus the arm current $i_{j,k}$ is expressed as

$$i_{u,k} = \frac{i_{dc}}{3} + i_{cir,k} + \frac{i_k}{2} \tag{2.2}$$

Switch State		SM terminal voltage	Arm current polarity	State of capacitor
S1	S2			
On	Off	V_c	+	Charging
Off	On	0	+	By-passed
On	Off	V_c	-	Discharging
Off	On	0	-	By-passed

Table 2.1: States of sub modules

$$i_{l,k} = \frac{i_{dc}}{3} + i_{cir,k} - \frac{i_k}{2} \tag{2.3}$$

where, $i_{cir,k}$ is the circulating current resulting from regulation of capacitor voltages in SMs.

The circulating current and the AC side current are calculated from Equation 2.2 and Equation 2.3 as

$$i_{cir,k} = \frac{i_{u,k} + i_{l,k}}{2} - \frac{i_{dc}}{3} \tag{2.4}$$

$$i_k = i_{u,k} - i_{l,k} \tag{2.5}$$

Based on Kirchoff's voltage law and Figure 2.1, the dynamic equations of MMC in phase k can be expressed as:

$$\frac{V_{dc}}{2} - v_{u,k} - R_{arm} i_{u,k} - L_{arm}\frac{di_{u,k}}{dt} - R_r i_k - L_r \frac{di_k}{dt} - v_k^G = 0 \tag{2.6}$$

$$-\frac{V_{dc}}{2} + v_{l,k} + R_{arm} i_{l,k} + L_{arm}\frac{di_{l,k}}{dt} - R_r i_k - L_r \frac{di_k}{dt} - v_k^G = 0 \tag{2.7}$$

Adding Equation 2.6 and Equation 2.7, and substituting ac side current i_k as given in Equation 2.5, the outer dynamic equations of MMC becomes:

$$(L_{arm} + 2L_r)\frac{di_k}{dt} = -(R_{arm} + 2R_r) i_k - v_{u,k} + v_{l,k} - 2v_k^G \tag{2.8}$$

After some simplifications Equation 2.8 can be written as:

$$L_{eq}^{ac}\frac{di_k}{dt} = V_k - R_{eq}^{ac} i_k - v_k^G \tag{2.9}$$

where L_{eq}^{ac} = $L_{arm}/2 + L_r$, R_{eq}^{ac} = $R_{arm}/2 + R_r$ and V_k = $(-v_{u,k} + v_{l,k})/2$. L_{eq}^{ac} and R_{eq}^{ac} indicate the equivalent inductance and resistance in the AC grid respectively

Subtracting Equation 2.7 from Equation 2.6 and substituting $i_{diff,k}$ given in Equation 2.4, the inner dynamic equation for MMC becomes:

$$L_{arm}\frac{di_{cir,k}}{dt} = \frac{V_{dc}}{2} - R_{arm} i_{cir,k} - R_{arm}\frac{i_{dc}}{3} - V_{cir,k} \tag{2.10}$$

where, $V_{cir,k} = (v_{u,k} + v_{l,k})/2$. According to Equation 2.9, the AC side current can be directly controlled by the difference between capacitor voltages in the upper and lower arms ($v_{u,k}$ and $v_{l,k}$) and according to Equation 2.10, circulating current can be controlled by the sum of these voltages. This is the basic theory used for the control of MMC.

2.3. Control of MMC

The controls required in a MMC-HVDC converter can be classified into three levels: lower level controls, upper level controls and dispatch controls as illustrated in Figure 2.3 [14]. Station or dispatch controls can be classified as the controls that manage the operating set points such as DC voltage (V_{dc}), active power (P), AC voltage (V_{ac}) or reactive power (Q) to meet both AC And DC system requirements. The dispatch controls provide set-points required by the upper level controls.

Upper level control generates the reference voltage wave for the lower level control. Upper level control has a response time of a few hundred milliseconds. The upper-level control has a decoupled inner current controller whose references are generated based on MMC operating mode defined by the dispatch controls. The control also depend on the type of MMC, grid following (non-island) or grid forming (island) as explained in section 2.4. The reference is generated by using vector control philosophy where the 3-ϕ ABC system quantities are transformed into DQ system quantities by Park's transformation. This is done to have a flexible and independent control of active and reactive power using simple DC parameters (in the DQ system) of their equivalent 3-ϕ parameters (in the ABC system).

Lower level control comprises of capacitor voltage balancing, circulating current suppression and IGBT switching pluses. These controls receive the voltage reference waveform as their main input. They are responsible for the development of firing pulses necessary to produce the AC waveform that were requested by the upper level control. The lower level control provides valve firing signals and ensures that cell capacitor voltage in each submodule (SM) remains constant according to a predetermined value. This is achieved by selectively switching SMs based on the direction of arm currents. However, this regulation of capacitor voltages results in circulating currents among the three-phase units. This current does not influence the currents in the AC and DC sides, but they distort the arm current and increase the rated current of the submodules. A control loop to suppress the circulating current is included to reduce these effects.

After applying Park's transformation to Equation 2.9 and Equation 2.10, the grid currents and circulating currents can be defined as [11]

$$\frac{di_{dq}}{dt} = \frac{1}{L_{eq}^{ac}}(V_{dq} - (\omega L_{eq}^{ac} J_2 + R_{eq}^{ac} I_2) i_{dq} - V_{dq}^{G}) \tag{2.11}$$

$$\frac{di_{cir,dq}}{dt} = -\frac{1}{L_{arm}}(V_{cir,dq} + (R_{arm} I_2 - 2\omega L_{arm} J_2) i_{cir,dq}) \tag{2.12}$$

where, V_{dq} and $V_{cir,dq}$ are modulated voltages in grid current and circulating current controller, respectively and ω the fundamental angular frequency. I_2 is the identity matrix with size 2×2, and $J_2 = \begin{bmatrix} 0 & 1 \\ -1 & 0 \end{bmatrix}$

Capacitor voltage balancing is the final stage of lower level controller. Firing pulses are generated to ensure uniform capacitor voltages across SMs within one arm. The sorting method is commonly employed for this purpose, wherein SM capacitor voltages are sorted from highest to lowest. Modulation indices are determined based on the upper-level and circulating current suppression control voltage references. Based on the sorting and modulation indices, the controller decides which SMs should discharge during negative arm currents (highest voltages) and which should charge during positive arm currents (lowest voltages). This method aids in maintaining balanced capacitor voltages and overall system stability.

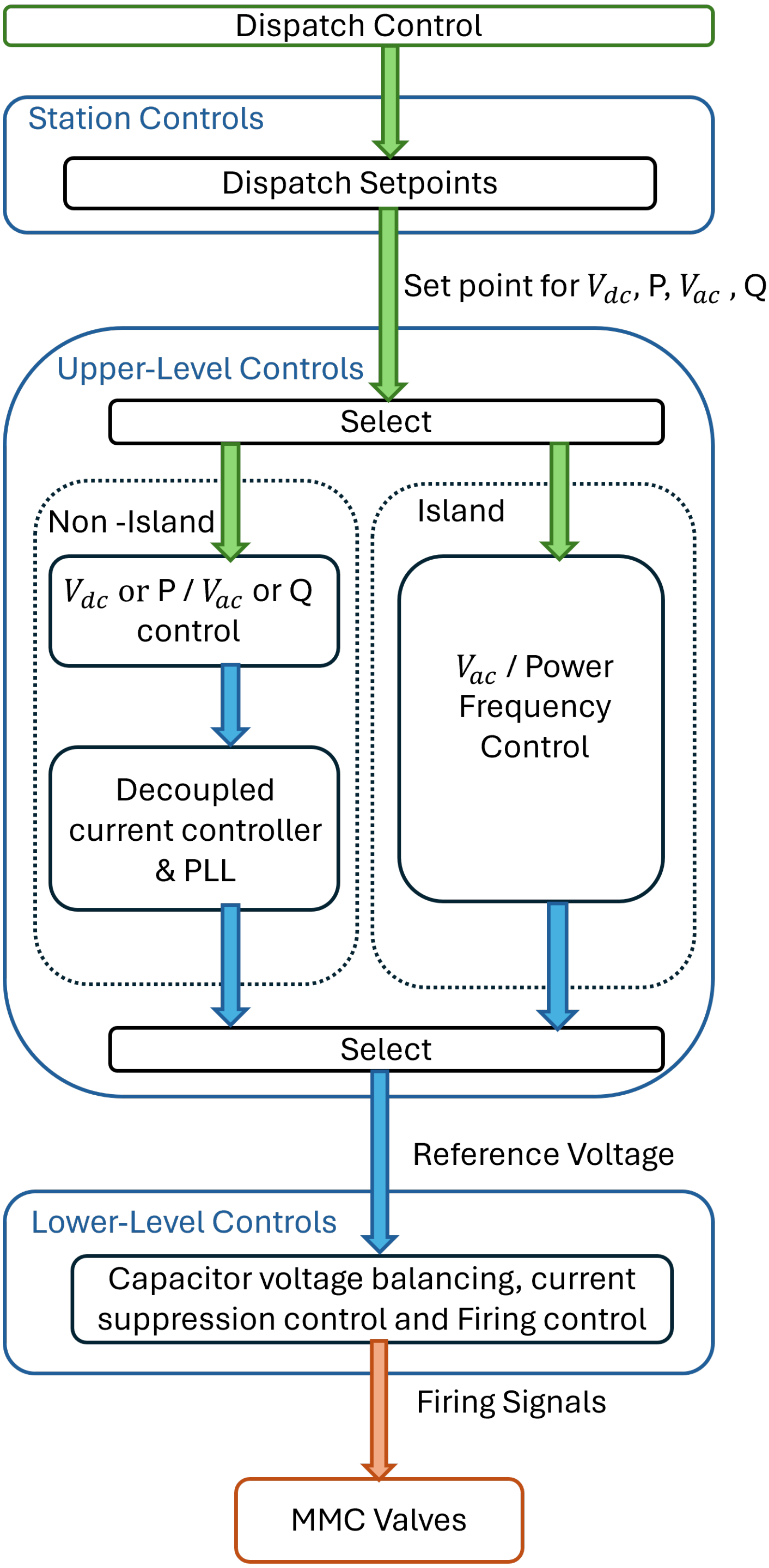

Figure 2.3: MMC control hierarchy

2.4. Grid following and grid forming converters

There are two main control strategy for MMC converters mainly grid following (GFL) control strategy and grid forming (GFM) control strategy. A simplified representation of grid following converter (GFL) and grid forming converter (GFM) are given in Figure 2.4 [17]. GFL converters are described as a unit whose behavior can be approximated to a controlled current source with high parallel impedance whereas GFM converters behave as voltage sources with low series impedance. GFL converters achieve power injection or voltage regulation by controlling injected currents, while GFM converter regulates by directly controlling voltage at its output terminal.

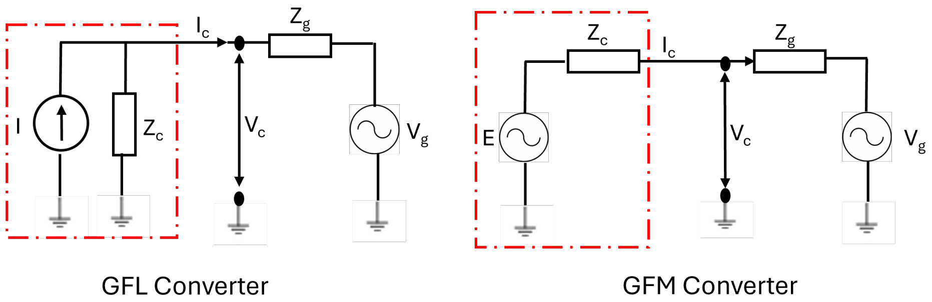

Figure 2.4: Simplified representation of GFM and GFL converters

When the converters are connected to strong grid environment, the grid dictates the voltage angle and magnitude of the converter controls. This setup, where the converter controls follow the voltage angle and magnitude inputs from a strong grid is known as GFL control strategy. GFL converter requires a dedicated unit to identify the grid voltage angle and calculate proper phase shift. This is done by means of phase locked loops(PLLs). They implement a dual-loop vector control strategy to regulate the active and reactive currents injected into the power grid.

One main concern with the increasing penetration of renewables is the impact on power system frequency stability. Renewable sources do not provide a positive response to frequency disturbances such as load fluctuations or to the loss of generating units within power grid. Hence it is crucial to enhance the dynamic frequency support capacity of renewable energy sources to maintain frequency stability. A power grid with high penetration of renewables often behaves as a weak grid due to lower reliability of renewable sources. When the converters are connected to weak grids, power fluctuations can cause significant variations in the grid voltage's magnitude and frequency, negatively impacting the performance of the PLL and associated control system [18]. This has led to the development of GFM control. GFM converters are responsible for establishing and regulating grid voltages at the point of common coupling (PCC), especially in islanded operation mode. The control objective is to stabilize grid frequency and regulate voltage amplitude. GFM converters are able to self synchronize to the grid without the need of a dedicated unit.

3

Fault Analysis: Asymmetrical faults

Maintaining a balanced operation is crucial for reliability and safety in electrical power systems. A power system network is considered balanced when it is operated under normal load conditions without any disruptions. However, various factors can disturb this equilibrium leading to faults. Among these, short circuit faults play a pivotal role. They occur when an unintended low-resistance connection is created between two points in an electrical circuit. This results in a rapid increase in current flow, which can have serious consequences if not addressed promptly. This chapter conducts a fundamental analysis of faulted networks between offshore MMC and wind plant using classical power system fault analysis method based on sequence components, particularly focusing on asymmetrical faults.

Short circuit faults are categorized into two main types: symmetrical and unsymmetrical faults. Symmetrical faults, such as three-phase short circuit faults (L-L-L) and three-phase to ground faults (L-L-L-G), affect all three phases equally. Despite the fault, the system remains in a balanced state as all lines are impacted symmetrically. Analyzing symmetrical faults is straightforward due to their balanced nature [19]. In contrast, unsymmetrical faults, including single line to ground faults (L-G), line to line faults (L-L), and line to line to ground faults (L-L-G), disrupt the balance of the system. These faults can lead to imbalances in voltage and current distribution across the network.

Majority of faults in power systems are asymmetrical. To analyze an asymmetrical fault, it is necessary to solve an unbalanced 3-Φ circuit. Directly solving this type of circuit is very challenging, but using symmetrical components simplifies the task by converting it into three single-phase networks. Sequence component analysis is essential to fault analysis as it simplifies the calculation of fault currents by breaking down the system's behavior into positive sequence, negative sequence, and zero sequence components [7].

Symmetrical components transforms three-phase a, b, c variables F^{abc} into equivalent variables F^{0+-} in sequence frame through power variant transformation as given in Equation 3.1 [8]

$$F^{abc} = AF^{0+-}; F^{0+-} = A^{-1}F^{abc} \tag{3.1}$$

where the transformation matrix A and its inverse are given by Equation 3.2 and Equation 3.3 respectively.

$$A = \begin{bmatrix} 1 & 1 & 1 \\ 1 & \alpha^2 & \alpha \\ 1 & \alpha & \alpha^2 \end{bmatrix} \tag{3.2}$$

$$A^{-1} = \frac{1}{3}\begin{bmatrix} 1 & 1 & 1 \\ 1 & \alpha & \alpha^2 \\ 1 & \alpha^2 & \alpha \end{bmatrix} \tag{3.3}$$

where $\alpha = 1\angle 120°$. The zero, negative and positive sequence voltages are given as:

$$V^0 = \frac{1}{3}(V^a + V^b + V^c) \tag{3.4}$$

$$V^+ = \frac{1}{3}(V^a + \alpha V^b + \alpha^2 V^c) \tag{3.5}$$

$$V^- = \frac{1}{3}(V^a + \alpha^2 V^b + \alpha V^c) \tag{3.6}$$

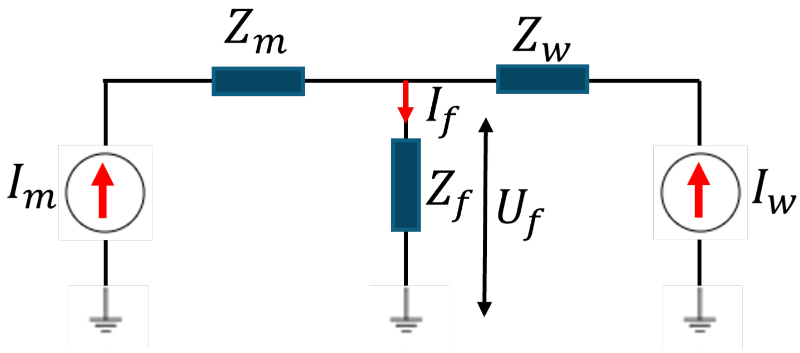

Figure 3.1: Generic network for fault analysis

Power converter-interfaced generation units function as controlled current sources in both the positive and negative sequence circuits in the event of an unbalanced fault. An asymmetrical fault is modeled between the lines connecting the offshore wind plant and offshore MMC in this study. The detailed description of the system considered is explained in chapter 4. Figure 3.1 gives an equivalent circuit with current sources modeled for wind plant and MMC to understand and analyse the asymmetrical fault [6]. In Figure 3.1, I_m and I_w represents the current sources of offshore MMC (OFFMMC) and wind plant (WP) respectively. The equivalent impedance from OFFMMC (transformer+line) is represented by Z_m and equivalent impedance from WP is given as Z_w. The fault current and fault voltage are given as I_f and U_f, respectively and the fault impedance represented as Z_f. Power circuits are decomposed into equivalent negative, positive and zero sequence circuits to analyse L-G, L-L and L-L-G faults [5, 6] as explained in subsequent sections.

3.1. Single phase to ground fault

The equivalent sequence network during a single phase to ground fault is given in Figure 3.2. The equivalent circuit implies that positive, negative and zero sequence components are in series, that is the positive, negative and zero sequence currents flowing into fault have to be equal and in phase to each other. The fault currents are given as:

$$I_f^+ = I_f^- = I_f^0 = I_m^+ + I_w^+ \tag{3.7}$$

3.2. Phase to phase fault

The equivalent sequence network connection for a phase to phase fault is given in Figure 3.3 where the zero sequence network does not appear. In phase to phase faults the positive and negative sequence components are connected in parallel, and they have equal magnitudes but opposite phase. The fault currents are given as:

$$I_f^+ = -I_f^- = I_m^+ + I_w^+ \tag{3.8}$$

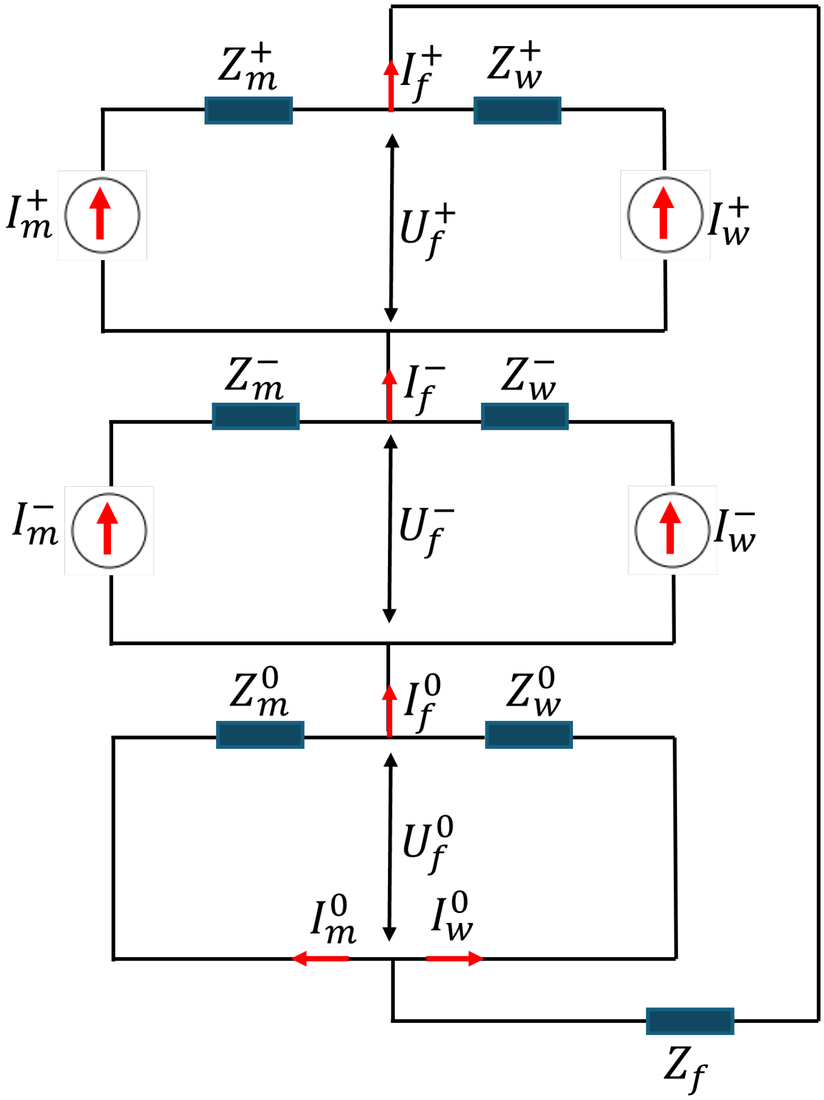

Figure 3.2: Sequence network equivalent for single phase to ground fault

3.3. Double phase to ground fault

The equivalent sequence network connection for phase to phase to ground fault is given in Figure 3.4. The circuit implies that the positive, negative and zero sequence networks are connected in parallel. The fault currents are given as:

$$I_f^+ = -(I_f^- + I_f^0) = I_m^+ + I_w^+ \tag{3.9}$$

Based on the sequence network analysis for various types of asymmetrical faults, several conclusions can be drawn. Fault current is provided by both wind plant and offshore MMC. The magnitude and phase of fault current depends on the magnitude and phase of the output current of OFFMMC and WP. For single phase to ground fault and phase to phase fault, suppression of negative sequence current means suppression of positive sequence currents. Hence it is not possible to suppress the negative sequence current of the OFFMMC and WP simultaneously. For phase to phase to ground fault, positive sequence current is the sum of negative and zero sequence current. This means that for this type of fault, suppression of negative sequence currents of OFFMMC and WP are possible. However a

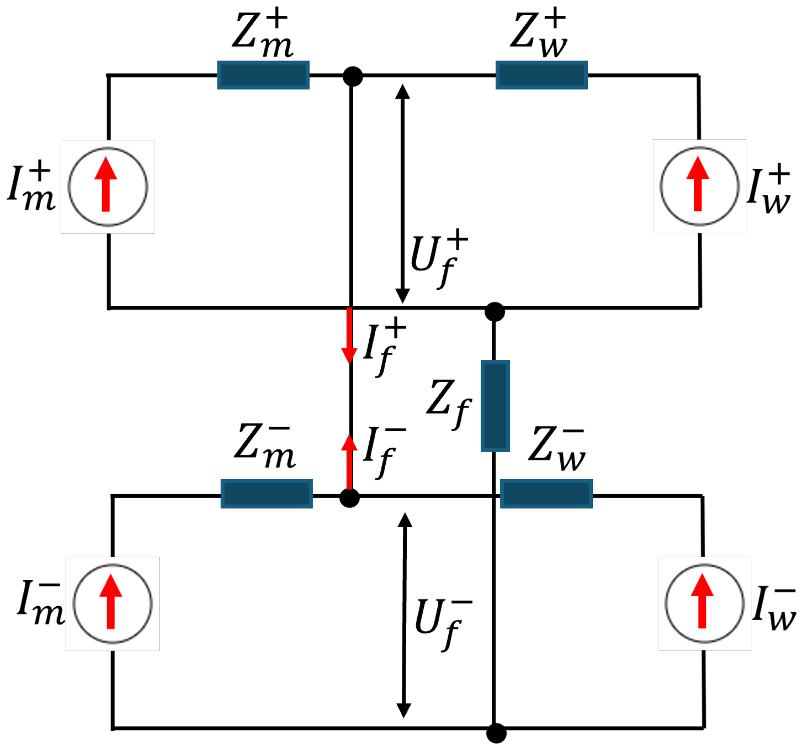

Figure 3.3: Sequence network equivalent for phase to phase fault

separate control algorithm to identify the type of fault will be required. Moreover, the configuration of the transformer also determines the flow of zero sequence current. In this study the transformer configuration adopted is YNd without a zero sequence path, thereby preventing the flow of zero sequence current into the converter. Hence the short-circuit current of each phase in system contains only positive and negative sequences [20]

Expanding further on the insights from fault analysis, the present study focuses on suppressing the negative sequence current only in the offshore MMC and follow the default controls for the wind turbine as explained in section 4.3. Limiting the negative sequence current of the OFFMMC is beneficial in reducing the large negative sequence currents generated in the system during asymmetric faults, thus helping to restore power system stability.

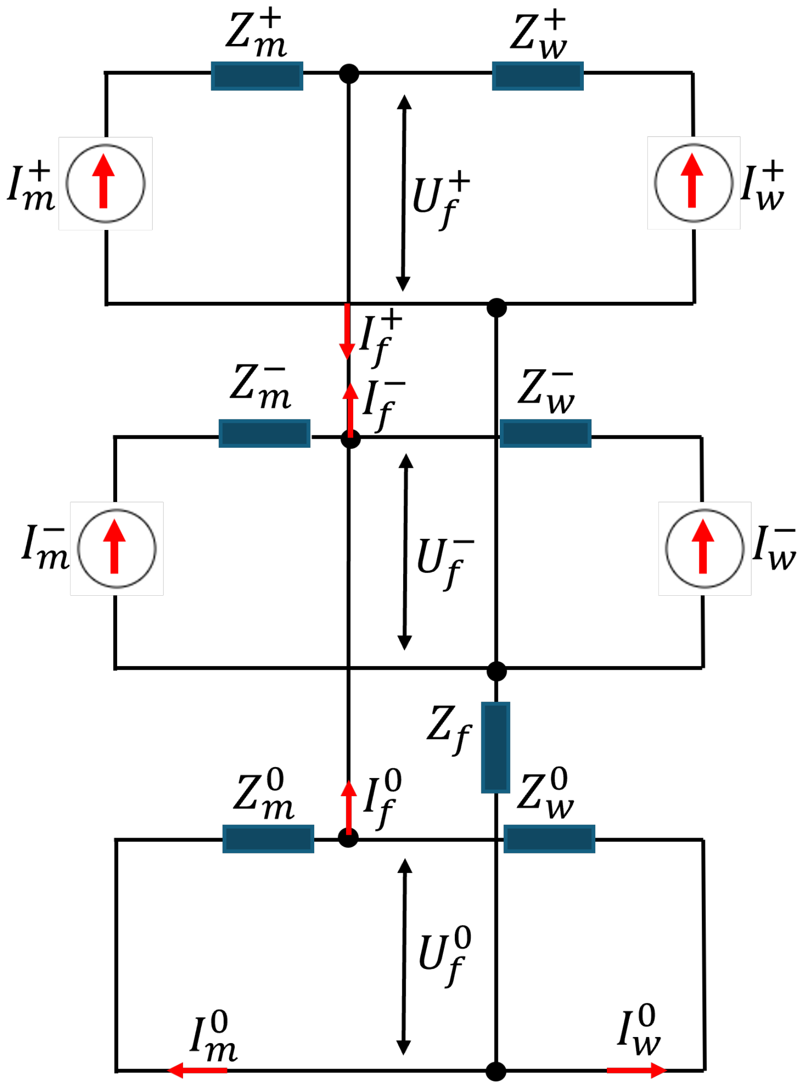

Figure 3.4: Sequence network equivalent for phase to phase to ground fault

4
System Description

This chapter provides an in-depth explanation of the multi terminal HVDC system utilized in this thesis to evaluate power system stability under asymmetrical faults. Detailed descriptions of the controls employed for different MMCs within the system are included. Additionally, the chapter offers an overview of the Real Time Digital Simulator (RTDS) and covers the process of modeling the power system within the RSCAD environment.

A three-terminal meshed MMC-HVDC system as illustrated in Figure 4.1 is used in this study. The system consists of an offshore wind plant, an offshore converter, and two onshore converters. The rated power of the MMC-HVDC system is 2GW and the rated voltage is ±525 kV. A bipolar configuration is used for HVDC in this study. Converters CSA1 and CSA3 are connected to strong AC grids and are classified as grid-following converters (GFL). These converters follow the voltage and phase angle of the grid. The offshore wind farms are connected to the DC grid through converter CSA2, which is classified as a grid-forming converter (GFM). GFM converters are responsible for establishing and regulating grid voltage and synchronizing grid frequency. A cable of 300 km in length and 400 km in length connect the CSA2 with CSA1 and CSA3 respectively. The onshore converters CSA1 and CSA3 are also connected via cables. DC circuit breakers (DCCB) are provided at the end of each cables.

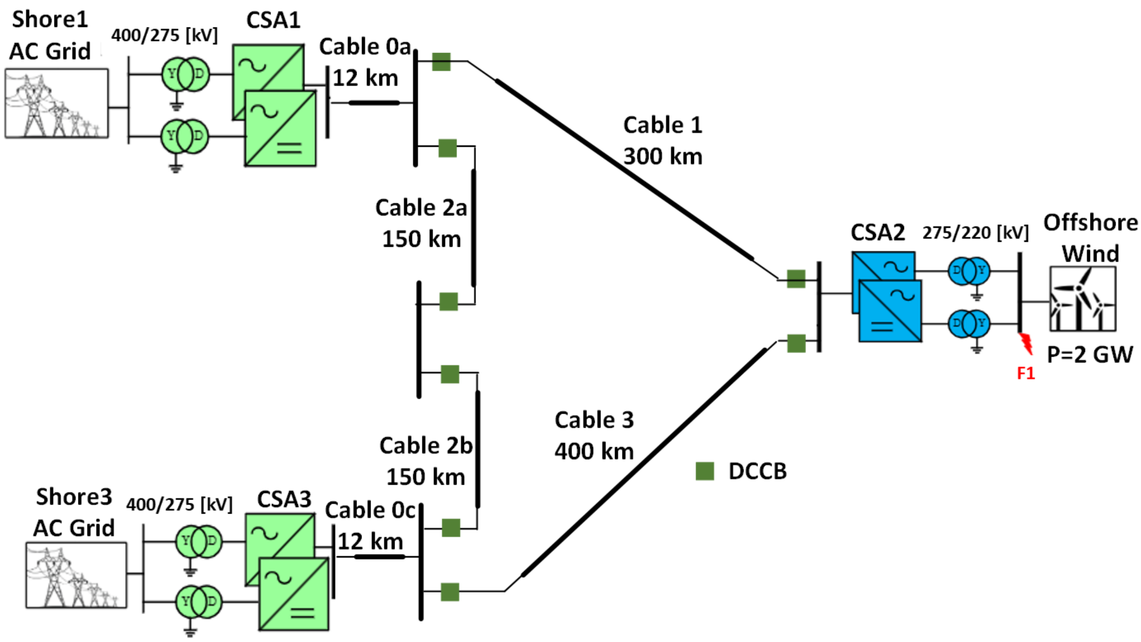

Figure 4.1: Configuration of the ±525 kV, 2GW, three-terminal MMC-HVDC system

4.1. Onshore Converter

The onshore converter, CSA1 acts as the slack converter controlling the DC voltage of the whole system. The control mode used is V_{dc}/V_{ac}, where the d-axis current reference $I_{d,ref}$ is controlled by the DC voltage loop and q-axis current reference $I_{q,ref}$ is controlled by AC voltage loop. Onshore converter, CSA3 uses control mode P_{ac}/Q_{ac} where the d-axis current reference, $I_{d,ref}$ is controlled by the active power loop and q-axis current reference, $I_{q,ref}$ is controlled by the reactive power loop. The control loops for CSA1 and CSA3 are shown in Figure 4.2. A Proportional-Integral (PI) controller is employed in the control algorithm to regulate the voltage, current and power signals. As mentioned earlier, CSA1 and CSA3 converters come under the GFL category. GFL converters require a dedicated unit to identify the grid voltage angle and calculate the appropriate phase shift. This is done using phase-locked loops (PLLs). The angle θ calculated from PLL is used for Park's transformation to convert three phase quantities (a,b,c) into two direct current (DC) quantities (d and q) as shown in Figure 4.3. This transformation simplifies the analysis and control of AC systems by converting sinusoidal quantities into steady-state DC quantities, making it easier to control and analyze the system dynamics in a rotating reference frame.

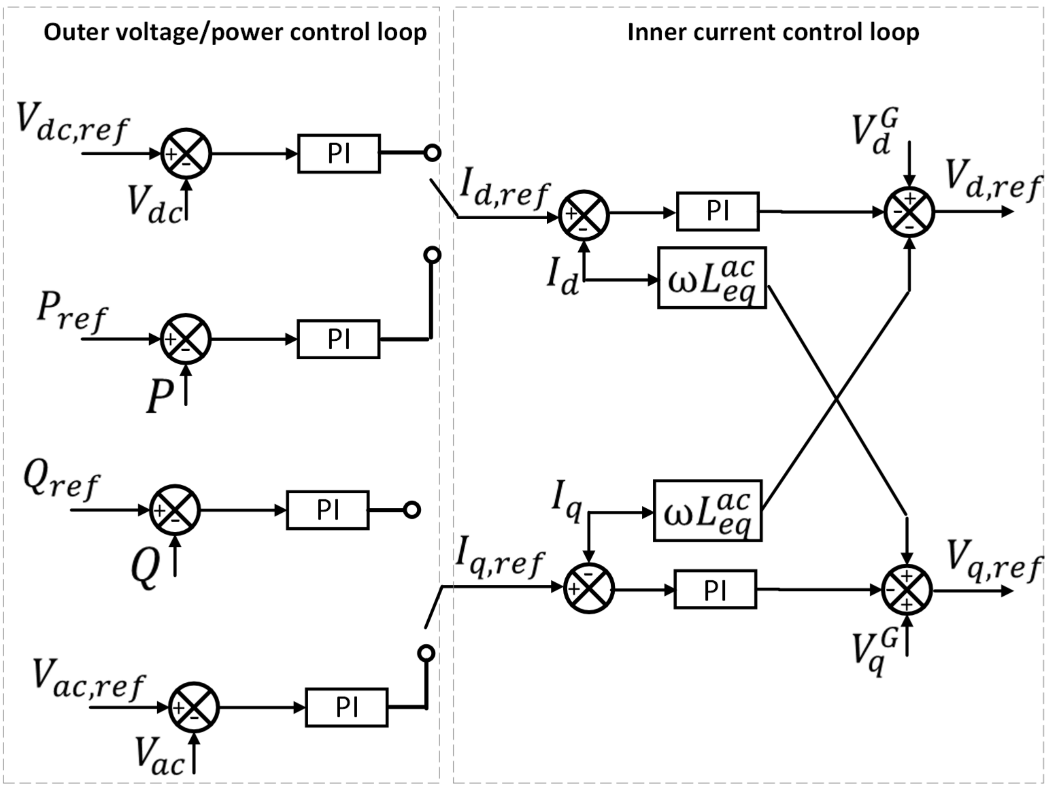

Figure 4.2: MMC control for grid-following converters

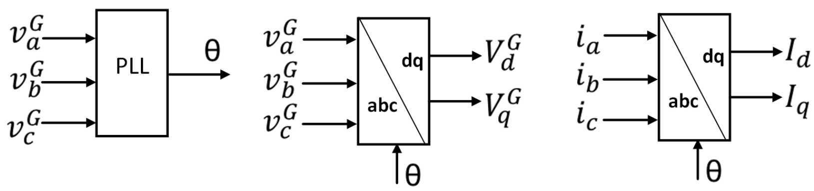

Figure 4.3: PLL & Park's transformation

The reference voltages from the outer level control as given in Figure 4.2 will be used to balance the capacitor voltages across all SMs. Difference in the arm phases of the MMC as a result of balancing of capacitor voltages produces circulating current. This current causes voltage ripples in SMs and distorts current through arm which influences rating of SM capacitance and IGBT switches. The circulating currents are associated with 2ω harmonics [12]. To minimize the effect of circulating currents, a suppression control is included as show in Figure 4.4. The d-axis and q-axis circulating currents I_d, cir and I_q, cir respectively are controlled to be zero.

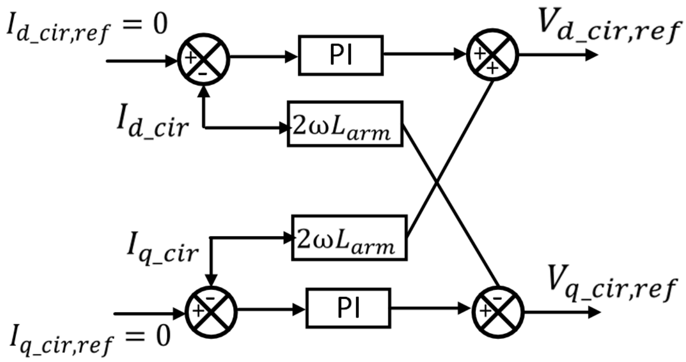

Figure 4.4: Circulating current suppression control

Modulation indices are determined based on the upper-level control voltage reference and the circulating current suppression control voltage references as given in Figure 4.5. These modulated indices determine the insertion or bypassing of SMs in each arm.

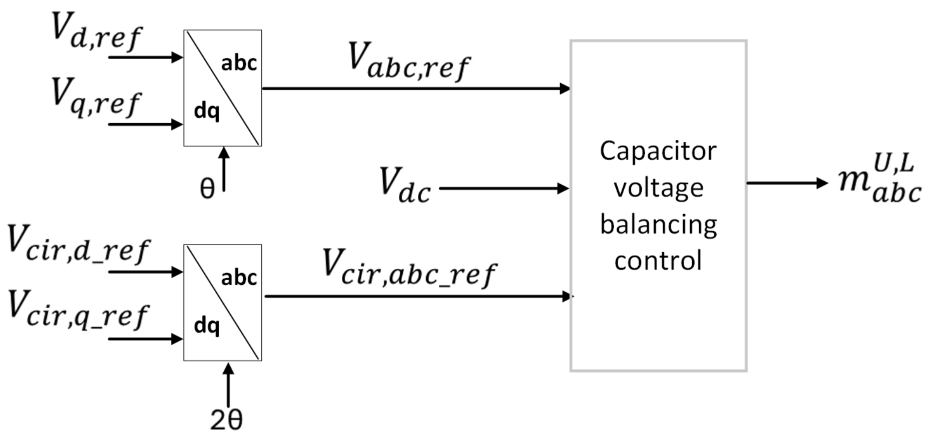

Figure 4.5: Modulation indices generation control

4.2. Offshore Converter

The offshore converter, CSA2 uses a grid-forming (GFM) control. GFM converters are responsible for establishing and regulating grid voltages at the point of common coupling (PCC), especially in islanded operation mode. The control objective is to stabilize grid frequency and regulate voltage amplitude. GFM converters can self-synchronize to the grid without the need for a dedicated unit. An overview of the different control algorithms for GFM converters is provided in [17]. Out of the variety of voltage control schemes developed, the simplest approach is to directly feed the voltage magnitude and phase angle which are generated from outer control loops to the modulation. The voltage amplitude is regulated as shown in Figure 4.6. However one drawback of this control scheme is the lack of current controllability which can lead to overcurrent tripping of the converter during grid faults.

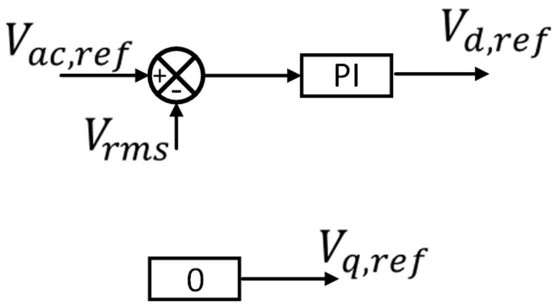

Figure 4.6: MMC control for offshore converter

In the event of an unbalanced fault, large negative sequence currents are generated in the system. A control strategy to mitigate the impacts of negative sequence currents is to suppress them. Given that this study focuses on offshore asymmetrical faults, control strategy specifically targets on suppressing the negative sequence current of the offshore converter, CSA2 as explained in chapter 3. The control algorithm given in Figure 4.6 is replaced with positive and negative sequence current control as given in Fig. 4.7-4.8 respectively. The positive sequence control focus on regulating the ac grid voltage and the negative sequence control focuses on suppressing the negative sequence currents. The proposed control strategy is triggered in the presence of a fault in the system, i.e., they are event-triggered. The sudden increase in negative sequence current acts as a fault detection mechanism in this study and serves as the trigger for implementing the proposed control strategy.

4.3. Offshore Wind Farms

Type 4 wind turbine (WT) is used in this study to model the wind plant. The wind turbine is integrated to the grid with the help of two full scale back to back converters connecting the stator of the PMSM to the grid as illustrated in Figure 4.9. The power extracted from the wind turbine can be represented as given in Equation 4.1 [21]

$$P_b = \frac{1}{2}\rho A v^3 C_p(\lambda, \beta) \tag{4.1}$$

where ρ is the air density in kg/m^3, $A = \pi r^2$ is the turbine swept area in m^2, r is the turbine radius in m and v is the wind speed in m/s. Function $C_p(\lambda, \beta)$ is the performance coefficient where λ is the tip-speed ratio and β is the blade pitch angle in degrees.

The VSC controls connected to PMSM (MSC) regulate the d-axis current to minimize the reactive power and improve the generator efficiency and regulates q-axis current to maximize the captured wind power. The q-axis reference current is generated from torque imposed on the machine. Torque is calculated based on the maximum power curve of the wind turbine as given in Equation 4.2.

$$P = k_{opt}\omega_r^3 \tag{4.2}$$

$$T = \frac{P}{\omega_r} = k_{opt}\omega_r^2 \tag{4.3}$$

where k_{opt} is the optimal power coefficient and ω_r is the rotor angular velocity. The optimal power coefficient is defined as

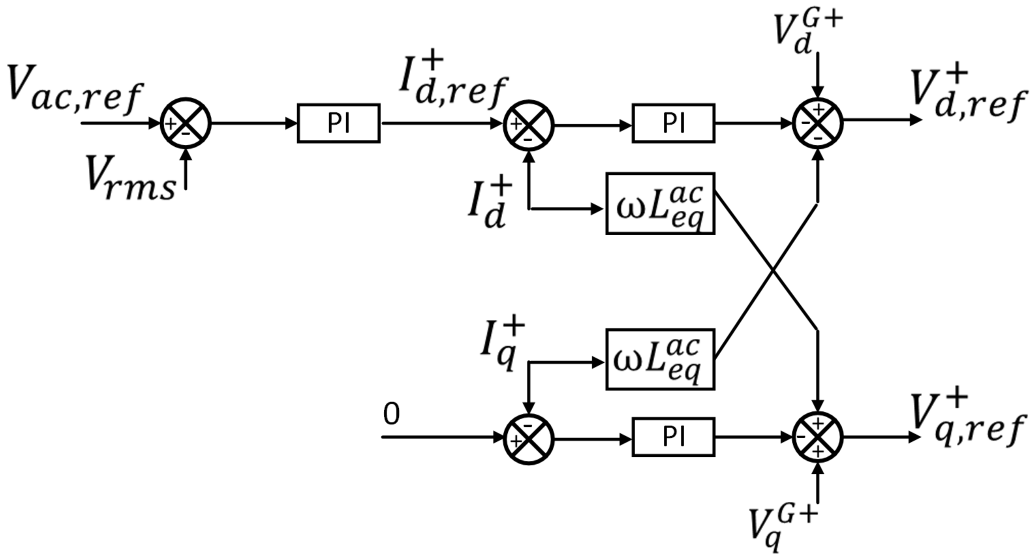

Figure 4.7: MMC offshore converter control - Positive sequence

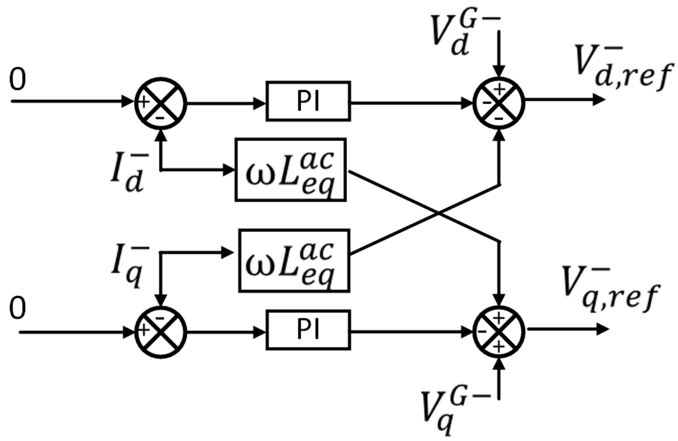

Figure 4.8: MMC offshore converter control - Negative sequence

$$k_{opt} = \frac{TR}{(GR.WR^3)} \tag{4.4}$$

where TR is the rated turbine power in MW, GR is the rated generator power in MVA and WR is the per unit generator speed at the rated turbine speed.

On the grid side, the DC voltage at the DC bus is controlled to ensure proper active power exchange between the generator and the grid. A user-defined DC voltage reference is used to maintain the balance between the incoming active power from the generator side and the outgoing active power to the grid side [18]. The VSC controls connected to the grid (GSC) regulates the d-axis current to maintain DC voltage and controls q-axis current to regulate the reactive power output.

4.4. Real Time Digital Simulator (RTDS) Model

RTDS simulators are specifically designed to perform real-time electromagnetic transient (EMT) simulation. It operates continuously in real time while providing accurate results over a wide frequency

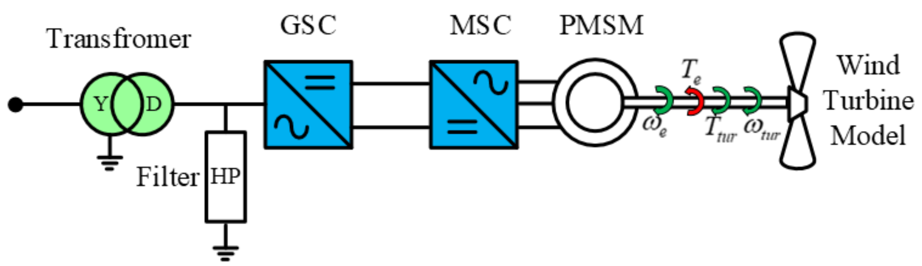

Figure 4.9: Type 4 wind turbine model

range. RTDS performs real time analysis of power systems using advance parallel processing techniques in order to achieve computational speeds, used for continuous monitoring of the power system. A powerful Graphical User Interface (GUI) called RSCAD is associated with RTDS. RSCAD has a large single and three phase power library along with different types of control methods used for power system troubleshooting and control.The fast continuous real time monitoring of RTDS for different systems makes it a powerful hardware used widely today in industry [22]. Real time power system simulation is especially useful for understanding the systems which are not yet implemented in real world like the 2GW HVDC connection considered in this thesis.

The three terminal meshed MMC-HVDC system representation in RTDS/RSCAD is given in Figure 4.10. The entire model is divided broadly into onshore and offshore indicating the onshore converter stations and the cables and offshore converter station and cables [23]. The model employs the dual time step technique available in RTDS to simulate power systems and power electronics components using different time steps. In this model, the converter stations are modeled in small timestep. Furthermore, 1 RTDS rack containing seven cores equipped with NovaCor processor is used to simulate the given MMC-HVDC system.

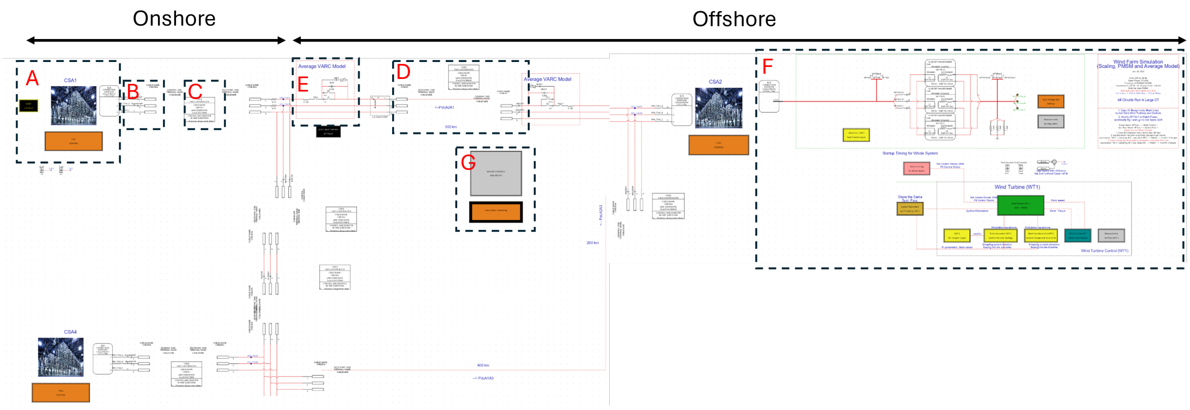

Figure 4.10: Thee terminal meshed MMC-HVDC system model in RTDS

In Figure 4.10, region A represents the converter station and connection between main and small timestep. It also consists of control & protection algorithms. In the given network, there are three such stations. Region B indicates the disconnector, which isolates the converter station from the land and sea cables. There are three disconnectors in the network. Region C consists of DMR (Dedicated Metallic Return) land cable, 20 km in length, connecting the onshore converter to the sea cable. There are two such land cables in the network. Region D comprises submarine cables, with a total of four cables in the network whose length are specified in Figure 4.1. Region E features the DC circuit breaker (DCCB), including fault logic and operating time of DCCB. Region F includes wind turbines and scaling transformers, simulating the wind farm. Region G contains general meters and master controls.

Further details of a converter station is given in Figure 4.11. It represents the small timestep environment of an onshore converter station. The converter station is divided into five regions for positive poles. Region I is an AC system with grid impedance to account for SCR impact. Region II region consists of the pre-insertion resistor. Region III is a star-delta transformer. Region V represents the the connection between the small timestep and the main timestep. Due to bipolar topology, there is an identical setup for the negative pole, except for regions I and V. Region I is not present in the offshore network, and there are two instances of region V. Region IV represents the MMC valves. The control section of the converter station includes the controls for positive and negative poles and protection schemes used in the study.

Various models are available in RTDS software to simulate MMC valves, each offering different benefits and trade offs. There are detailed models such as U5 and General Model (GM) which provide high accuracy and detailed dynamic representation, but require extensive hardware. There is also a simplified model that require reduced hardware requirements. For the present study, the simplified model available in RTDS is used. This model assumes the internal balancing of each submodule's (SM) capacitor voltages, eliminating the need for specifying which SMs to insert. Instead, it only requires the total number of SMs to be inserted. The control input is simplified to an overall deblock integer signal and the specified number of SMs to be inserted.

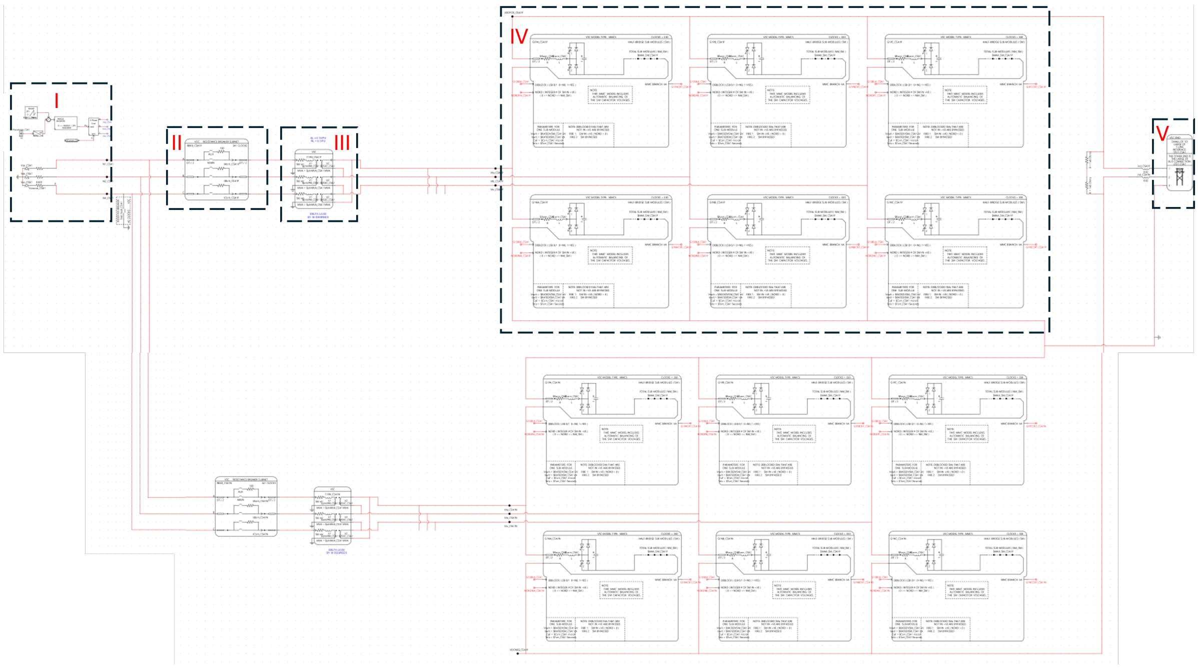

Figure 4.11: Small timestep environment of an onshore converter station

The wind turbine model in RSCAD is given in Figure 4.12 [21]. In order to maximize the turbine power generation, pitch angle must be set to optimal. If the power generation is below the nominal value, pitch angle is set to zero and if the wind speed is higher than the nominal value, the blades are pitched to limit the rotor speed and the power extracted from the wind. A proportional controller is used to control the pitch angle based on the wind speed. The torque value output from the wind turbine is input to the PMSM model as shown in **??**. Depending upon the torque input to PMSM, the stator power generator is transferred to the grid with the help of power electronic converters.

The wind turbine system model within RSCAD consisting of the PMSM, two back to back converters, DC capacitors and the interface transformers are illustrated in Figure 4.14. The primary focus of the

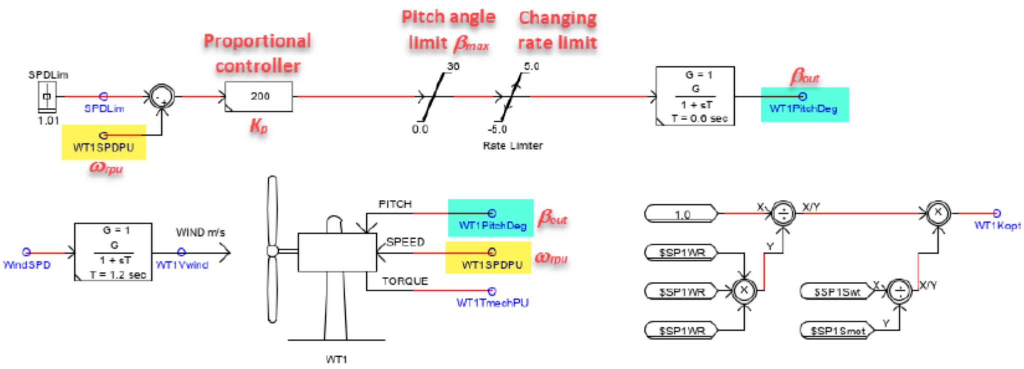

Figure 4.12: Wind turbine model including pitch angle control

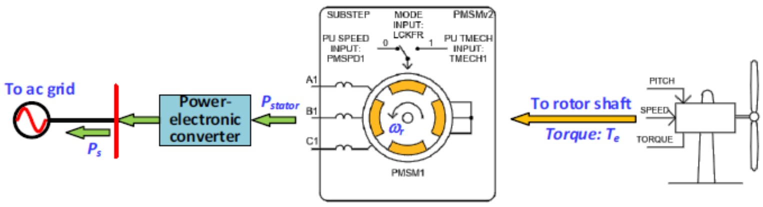

Figure 4.13: Power flow diagram from WT To grid

model is the control of the grid side converter and the PMSM side converter. The PMSM is modelled as an interior magnet machine, with sinusoidally distributed windings. Damper windings are ignored. The rated power is 2 MW. A 2-level VSC is used as the PMSM side rectifier and the grid side inverter. The various controls for the converters are covered in section 4.3

A suitable cable rating is required to link the offshore wind farms to the onshore grid system. Based on the type of travelling wave model used, different choices available to model DC cables are Bergeron and Frequency Dependant Phase models. The Bergeron model is based on a distributed LC parameter travelling wave line model, with lumped resistance. For accurate transient responses, it is important to model the DC cable as a frequency dependent line rather than a Bergeron line. The submarine XLPE cable is used and modeled within RTDS environment using frequency dependent model (phase domain). There is no frequency dependent travelling wave model in the small time step library due to the calculation burden of this model. As a result, the frequency dependent cable from the large time step library is used and interface t-lines are inserted to connect the DC cable in the large time step to the DC side of the MMC converter in the small time step. The interface line is a Bergeron model with an approximate cable length of 10 km. The DC cable length was modified to compensate for addition of the interface lines.

Power-electronic equipments are vulnerable to AC and DC faults. To protect these equipments from high fault currents and to improve the performance of power system, circuit breakers and protection measures are included in the system. DC faults should be detected within 2ms and the fault currents should be interrupted almost instantly. VSC-assisted resonant current (VARC) DCCBs are selected and implemented at each cable termination due to their rapid interruption speed [11]. DC overcurrent protection is also included in the model. The control circuit will enable a flag when the DC current goes above 6kA for 0.0001 seconds. The flag signal will force the converter valves to block and open the main AC breakers.

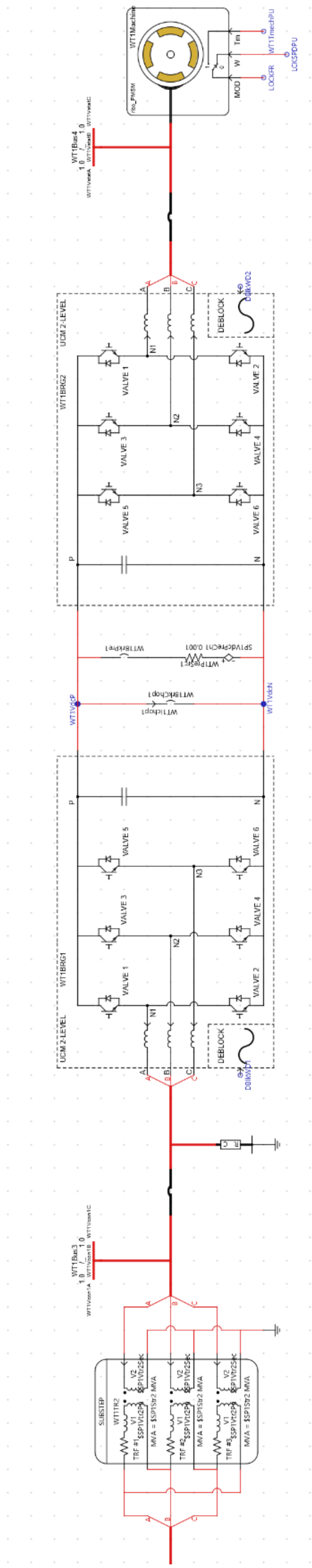

Figure 4.14: Wind turbine system

5
Linear and Non-linear controllers

The selection of control strategies plays a crucial role in achieving the desired system performance. chapter 4 delves into the various control algorithms used in the MMC-HVDC system to manage the evacuation of generated wind energy to the main grid. The objective is for the control to effectively operate the MMC-HVDC systems during different operational transients such as power flow changes, wind speed variations, and DC/AC grid faults. An effective controller should demonstrate faster settling times and minimize voltage and power variations during any transient in the system. The different control strategies for the MMC, as explained in chapter 4, are based on the state-of-the-art Proportional-Integral (PI) controller. PI controller is a linear controller widely adopted for their simplicity and effectiveness in regulating linear systems. MMCs have a variety of control variables and non linear dynamic equations, resulting in a non linear behavior of MMC [12]. Numerous studies have underscored the advantages of employing non-linear controllers over conventional PI controllers to enhance power system performance. This chapter provides an overview of the PI controller as well as the non linear controller Super twisting sliding mode controller(STSMC).

5.1. PI Controller

The proportional-integral control is the most commonly used control method because of its simplicity and robustness. The PI controller is a combination of proportional and integral functions designed to make the error signal converge to zero. The control function for PI is given as

$$u(t) = K_p e(t) + K_i \int e(\tau) d\tau \tag{5.1}$$

where K_p is the proportional parameter and K_i is the integral parameter. $e(t)$ is the error signal obtained from the difference between measured value of the signal $y(t)$ and the reference value $y^*(t)$ and $u(t)$ is the controller output. The proportional and integral parameters are chosen such a way that the output from the controller ensures minimization of the error signal.

The proportional gain is utilized to minimize errors, while the integral gain is responsible for driving errors towards zero by considering the historical accumulation of error values. $K_p e(t)$ generates an output proportionate to the current error. The proportional term functions with the steady-state error, which represents the difference between the desired reference value and the actual value. The integral term $K_i \int e(\tau) d\tau$ is directly related to both the size and duration of the error. It accelerates the convergence of the actual value towards the reference value and eliminates any residual steady-state error that might persist with a pure proportional controller. Integral term makes the controller sensitive to small errors. This compliments the proportional control action [24]

5.2. STSMC controller

Due to the non linear behavior of MMC, many studies have focused on non-linear controllers. The authors in [11, 25] explain the different non-linear controllers such as Model Predictive Control (MPC), Back-Stepping Control (BSC), and Sliding Mode Control (SMC). Out of the three, SMC has the benefit of high robustness against system uncertainties and fast transient response. However, the chattering problem of SMC can lead to system oscillations [26]. A second-order SMC, super twisting sliding mode controller (STSMC), has become popular recently, which not only preserves the robustness of the classical SMC but also overcomes the chattering issue.

In the SMC controller, a sliding surface is defined such that it guides the system states towards desired values. This sliding surface is typically based on tracking error, with the goal of minimizing this error to zero. When the states reach this surface, the controller uses a sign function to maintain the condition, which can lead to chattering phenomena due to the discontinuous nature of the sign function. Higher-order SMC such as STMSCs, are used to address the chattering issues by introducing an integral function in the sliding surface and improve the performance of the controller.

The sliding surface $\dot{S}$ for STSMC is proposed as outlined in Equation 5.2 [11]. The value of x is determined using the error signal obtained from comparing the measured actual value $y(t)$ to the reference value $y^*(t)$ as given in equation (5.3). Since both the terms of the sliding surface are continuous, the chattering is reduced. STSMC has PI controller internally which makes the controller very stable.

$$\dot{S}(y) = -\alpha\sqrt{(}x)\,\text{sgn}(x) - \beta\int(\text{sgn}(x)), \alpha, \beta > 0 \tag{5.2}$$

$$e = y^*(t) - y(t), x = K_i\int e + K_P e, \tag{5.3}$$

where $\alpha = 1.5\sqrt{H}$ and $\beta = 1.1H$. H is the upper bound of system disturbance. For this study, the value of H is set to 10.

The non linear controller, STSMC is implemented instead of the PI controller as given in Figure 5.1 and Figure 5.2 in the inner current loop of offshore converter, CSA2 for regulating sequence components in the presence of an unbalanced fault. If the inner loop is resolved quickly using non linear controller, the outer loop can be subsequently processed using the state-of-the-art PI controller. The remaining control loops, including circulating current suppression control, and onshore converter control loops, continue to utilize PI controllers.

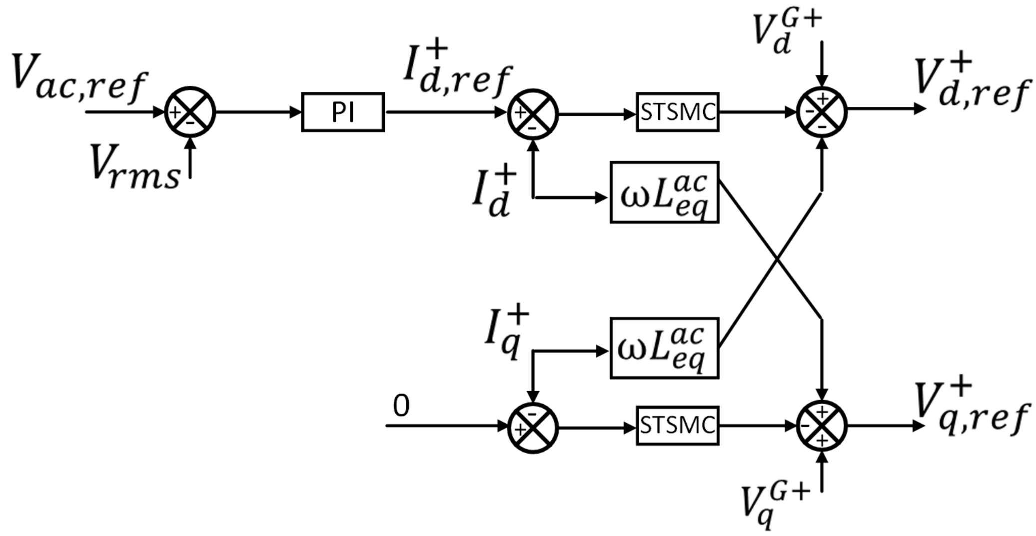

Figure 5.1: MMC offshore converter control(STSMC) - Positive sequence

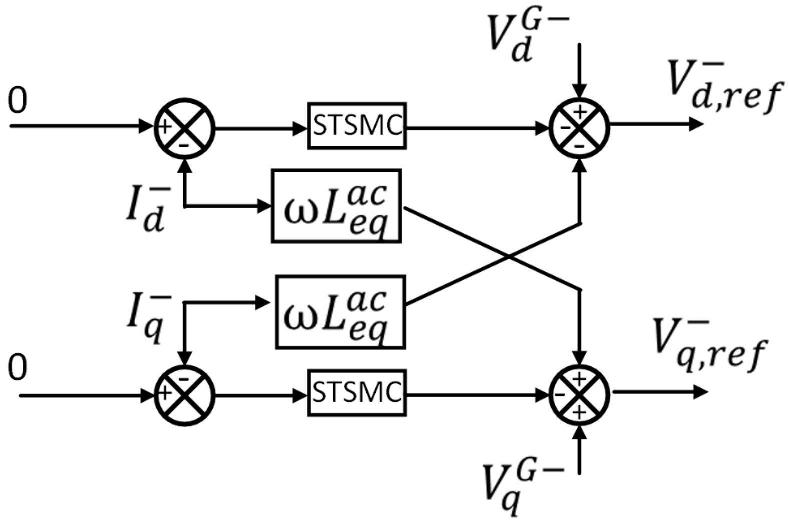

Figure 5.2: MMC offshore converter control(STSMC) - Negative sequence

6
Simulation Studies

In this chapter, we delve into the simulation studies conducted to investigate the fault ride-through capability of MMC based HVDC systems connected to offshore wind farms. Simulations are performed on a three-terminal meshed MMC-HVDC system connecting an offshore wind farm to two onshore AC grid as illustrated in Figure 4.1. The simulations studies are conducted using the Real Time Digital Simulator (RTDS), which accurately captures the transient response of the system, and assess the performance of control strategies in real time.

The transient response of the power system under various asymmetrical faults, including line-to-ground (L-G), line-to-line (L-L) and line-to-line-to-ground (L-L-G) faults are analysed. Initially, the behavior of the power system during offshore asymmetrical faults is investigated using the default controls. The characteristics of sequence components of current and voltage are analysed to detect and classify different faults. Subsequently, the effectiveness of the suppression of negative sequence control in offshore MMC in restoring system stability is evaluated using both PI controller and STSMC.

Table 6.1 provides details of the control mode and the parameters considered for the MMC converters. As illustrated in Figure 4.1, the fault occurs on the line connecting the offshore wind plant and the offshore MMC (CSA2). It is assumed that the AC fault will clear on its own after 300 milliseconds. A fault resistance of 0.001 Ω is considered. It is assumed that the fault currents are not high enough to activate the protection system modeled.

Table 6.1: Control mode and parameters of MMC converters

Parameter	**Converters**		
	CSA 1	**CSA2**	**CSA3**
Control mode	V_{dc}/V_{ac}	V_{ac}/f	P_{ac}/Q_{ac}
Rated active power [MW]	2000	2000	2000
AC Grid Voltage [kV]	400	220	400
DC link Voltage [kV]		$\pm$525	
Number of Submodules per arm		200	
MMC arm inductance [mH]		39.7	
MMC arm capacitance [μF]		15000	
Transformer leakage reactance [pu]		0.18	
AC converter bus voltage [kV]		275	

6.1. Baseline

Initially, the system employs the default voltage magnitude and phase angle control for offshore MMC, CSA2. To assess the system performance, the most severe fault scenario, L-L-G, is chosen. The fault occurs approximately at 2.5 seconds and is cleared around 2.8 seconds. The DC link voltage and active power signal for the different converters are given in Figure 6.1. It is observed that once the fault is cleared, the system remains unstable and the default control is not able to restore the system stability. Another observation is that the active power of the onshore converter CSA3 is maintained at 1GW. This is due to the user defined P/Q control assigned to CSA3.

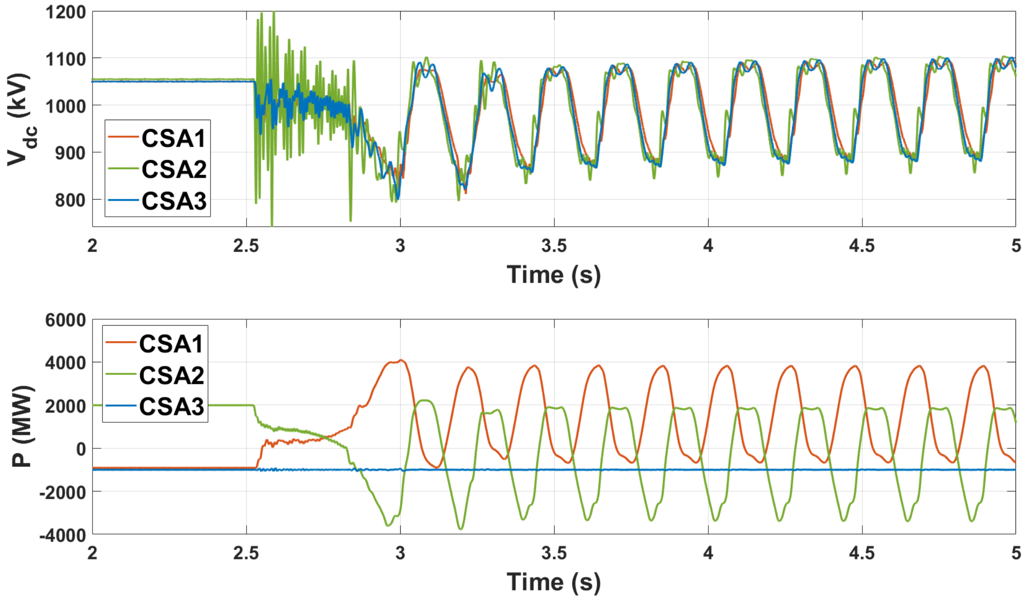

Figure 6.1: DC link voltage and active power plots for different MMCs with default controls during L-L-G fault

The positive, negative, and zero sequence current components in offshore converter, CSA2 during the fault are given in Figure 6.2. It can be observed that when the fault occurs at approximately 2.5 seconds, there is a significant increase in negative sequence currents. Although these negative sequence currents drop to nearly zero once the fault is cleared, around 2.8 seconds, the system does not stabilize. Additionally, it is noted that while grounded faults typically generate zero sequence currents, the transformer configuration in this case prevents any zero sequence current from flowing. The positive sequence current increases along with the negative sequence current.

6.2. Detection and classification of faults

Sequence components of current and voltage during faults are used to detect and classify different types of asymmetrical faults. The sudden increase in negative sequence current serves as a fault detection mechanism, triggering the proposed control strategy. This control strategy is designed to remain active for a specified duration, after which it reverts to the original voltage magnitude and phase angle control once the system is stabilized. The duration for which the control strategy is implemented depends on the type of asymmetrical fault (L-G, L-L, or L-L-G). The more severe the fault, the longer it takes to stabilize the system, thus extending the period during which the controller is active. This highlights the importance of accurately classifying different types of faults.

The positive, negative, and zero sequence voltage components during L-L-G, L-L and L-G faults are illustrated in Figure 6.3, Figure 6.4, and Figure 6.5 respectively. Due to the transformer configuration, zero sequence current is absent even in the case of grounded faults, as seen in Figure 6.2. However, this configuration results in a zero sequence voltage component in the presence of grounded faults, as shown in Figure 6.3 and Figure 6.5. This signal is used to differentiate between grounded and non-grounded faults. Now, to differentiate between the grounded faults L-G and L-L-G, the characteristics of sequence voltage components are utilized. Comparing the positive sequence voltages for faults

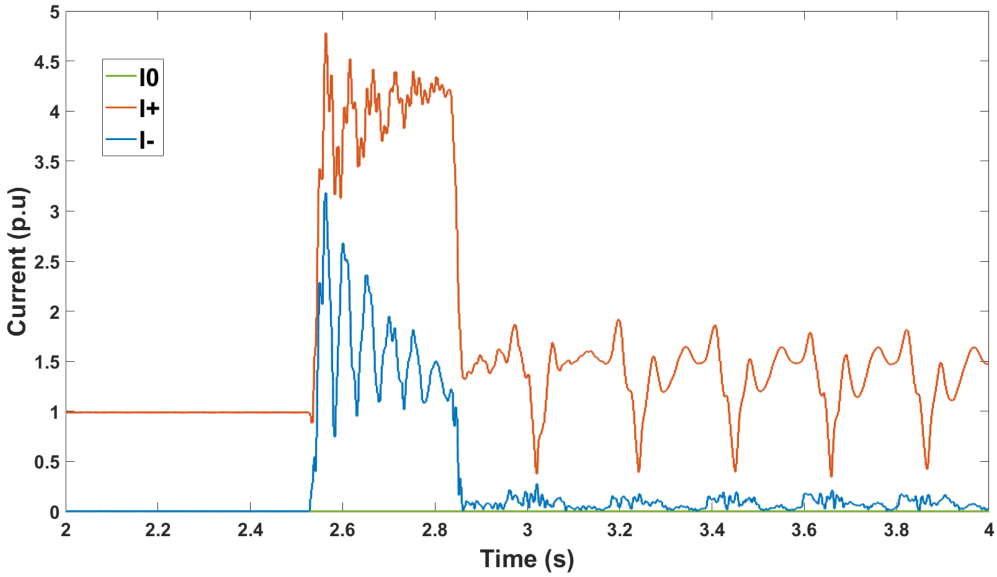

Figure 6.2: Positive, negative and zero sequence current signals during L-L-G fault

involving two phases and a single phase, it is observed that the decrease in positive sequence voltage is greater in two-phase faults than in single-phase faults.

Based on these observations, a classification rule is established as shown in Figure 6.6 to identify different types of faults. First, the presence of a fault is detected by comparing the negative sequence current across two time steps; if the difference exceeds a set limit, a fault is indicated. The value considered in this study is 0.45 p.u. Once the fault is detected, the zero sequence voltage is analyzed to distinguish between grounded and non-grounded faults. For practical implementation, the magnitude of zero sequence voltage is compared against a very small value (0.01 p.u). If the zero sequence voltage is less than the given value, it indicates L-L fault. To further differentiate between L-L-G and L-G faults, the magnitudes of the positive sequence component is compared against a threshold value. The value considered in this study is 0.48 p.u. This is done when the magnitude of zero sequence voltage is more than the positive sequence voltage to distinguish between L-G and L-L-G faults.

6.3. Sequence current control:PI controller

Utilizing the sequence components of current and voltage to detect and classify fault, negative current suppression control scheme is activated upon fault occurrence. The DC link voltage and active power signals for different faults (L-L-G, L-L, and L-G) using the conventional PI controller are given in Figure 6.7, Figure 6.8 and Figure 6.9. It is evident that with the introduction of negative sequence current suppression control, the system reverts back to a stable state post fault clearance. The control takes a few milliseconds to activate, as the algorithm must first detect an increase in negative sequence current and classify the type of fault before triggering the control scheme. This delay can account for the significant variation in DC link voltage observed at the moment the fault occurs. Due to its severity, the L-L-G fault necessitates a longer period for the system to stabilize compared to less severe faults. The negative sequence current plot of CSA2 for L-L-G fault is plotted in Figure 6.10. The control is able to minimize the negative sequence current once activated. The control remains active for a delayed duration even after the fault is cleared to help stabilize the system. We also observe a slight increase in negative sequence voltage around 3.6 seconds when the control is switched back to the original

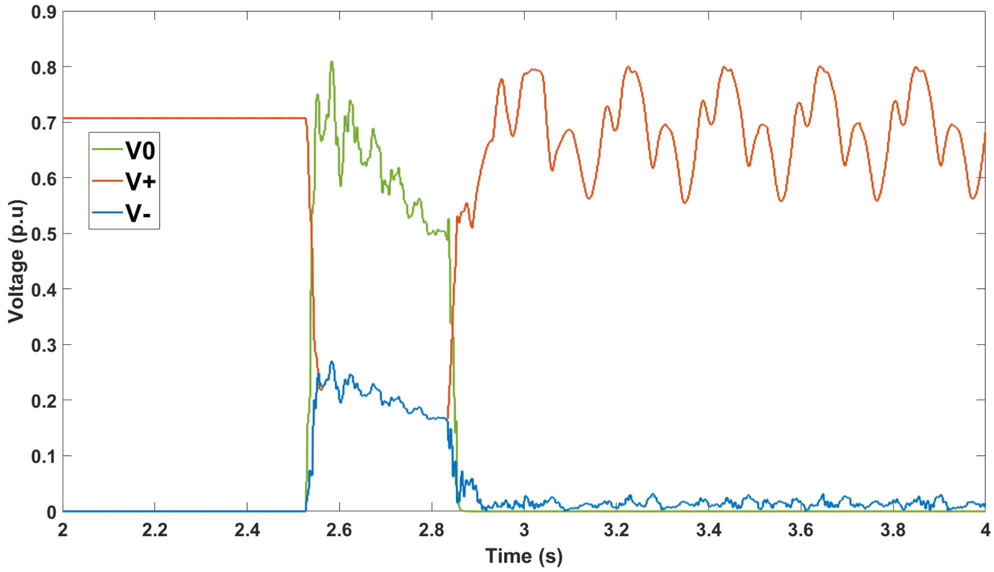

Figure 6.3: Positive, negative and zero sequence voltage signals during L-L-G fault

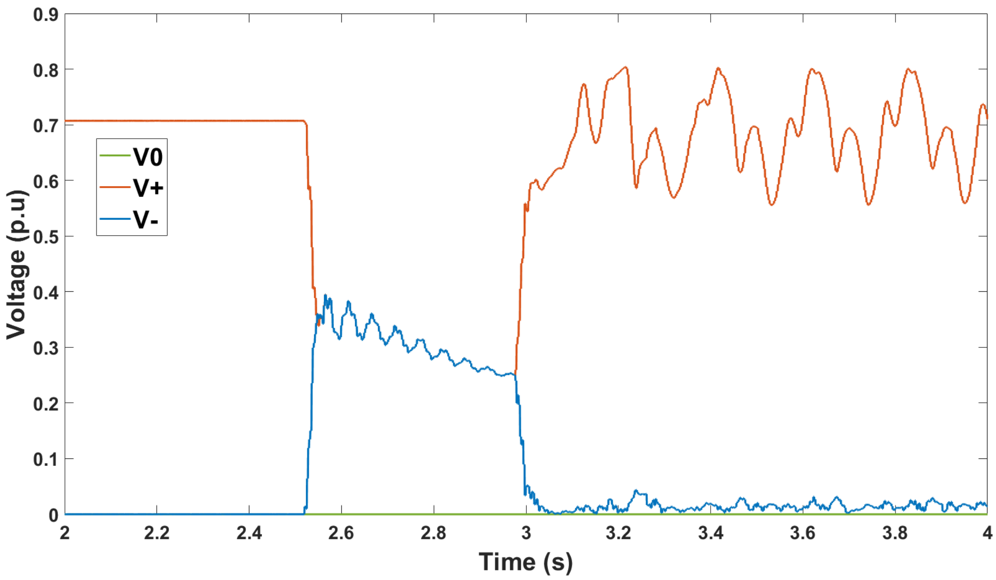

Figure 6.4: Positive, negative and zero sequence voltage signals during L-L fault

voltage amplitude and phase angle control.

6.4. Sequence current control:STSMC controller

Next, the traditional PI controller within the inner current control loop is substituted with STSMC for regulating sequence components in the offshore MMC, CSA2. Once the inner loop resolves quickly using STSMC, the outer loop can be subsequently processed using the PI controller. The remaining control loops, including circulating current suppression control, and onshore converter control loops, continue to utilize PI controllers.

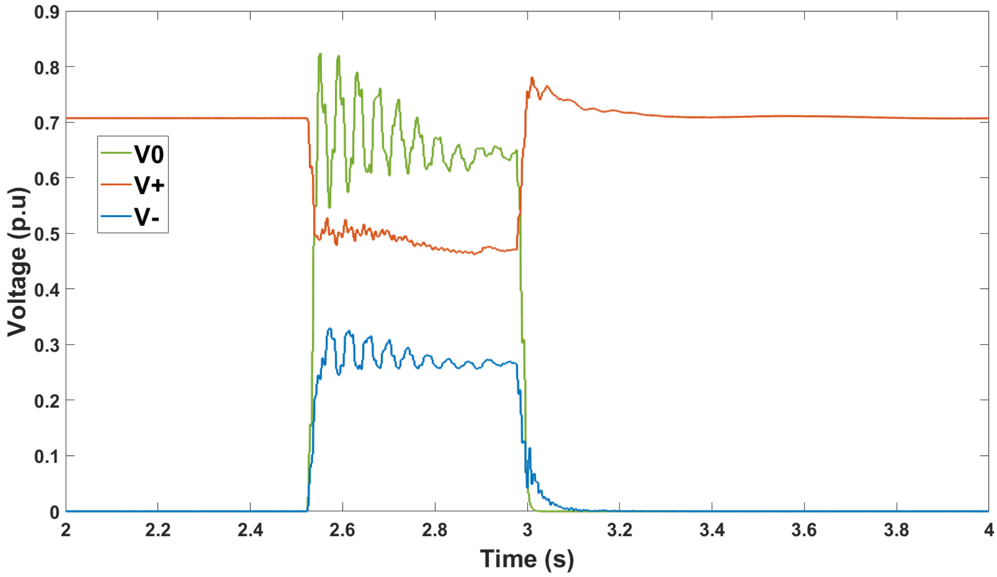

Figure 6.5: Positive, negative and zero sequence voltage signals during L-G fault

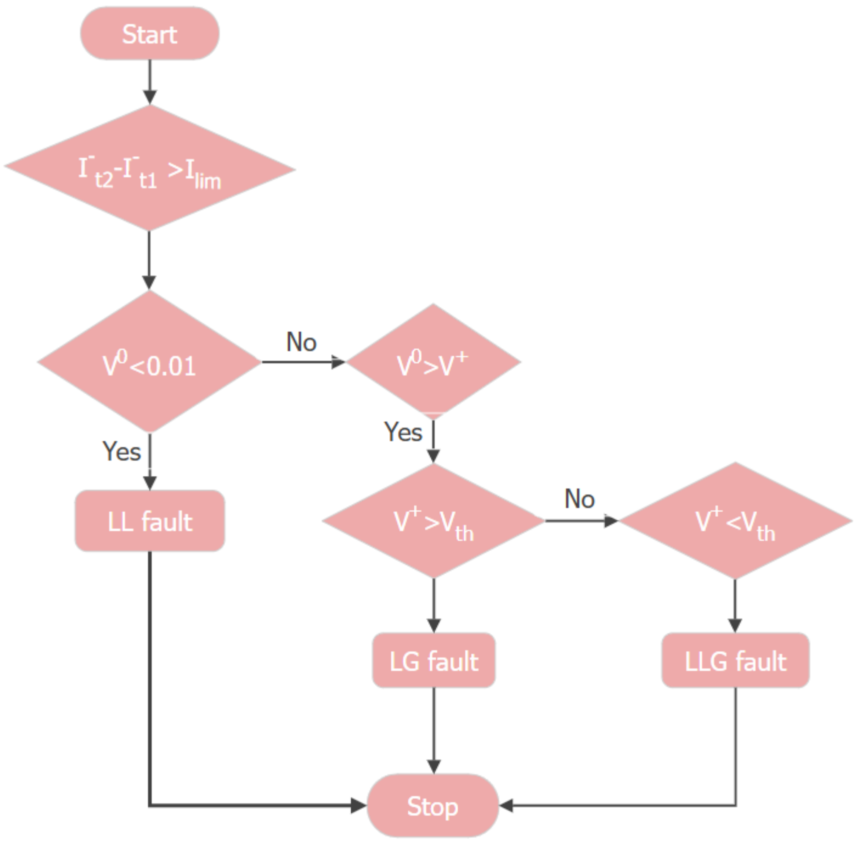

Figure 6.6: Classification of faults

The DC link voltage and active power signals for different faults using STSMC for the inner current loop are given in Figure 6.11, Figure 6.12 and Figure 6.13. Non-linear controller (STSMC) helps to restore the system back to its stable state quickly irrespective of the type of fault. This is a result of quicker

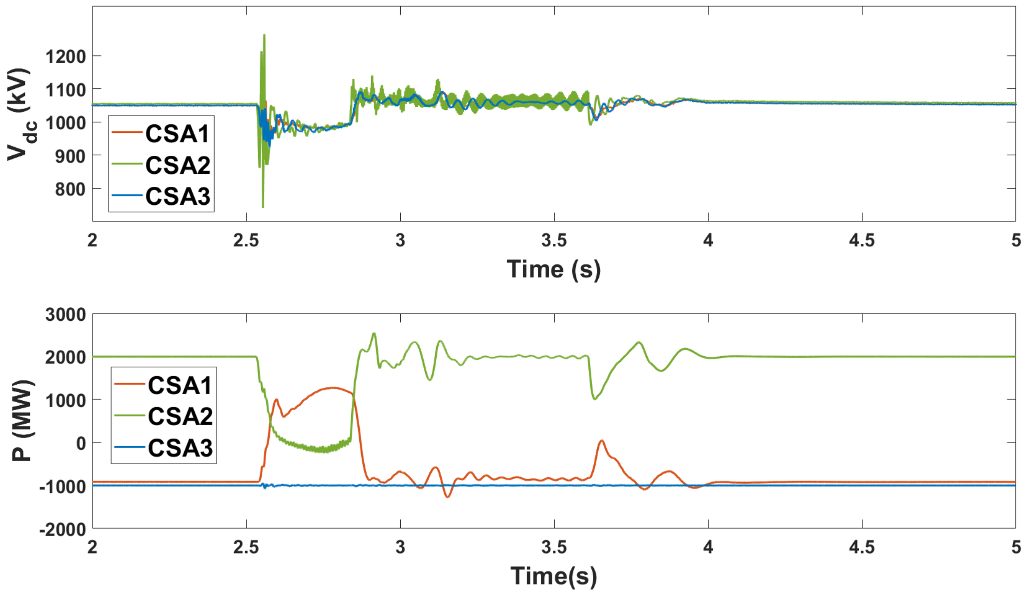

Figure 6.7: DC link voltage and active power plots for different MMCs during L-L-G fault using PI controller

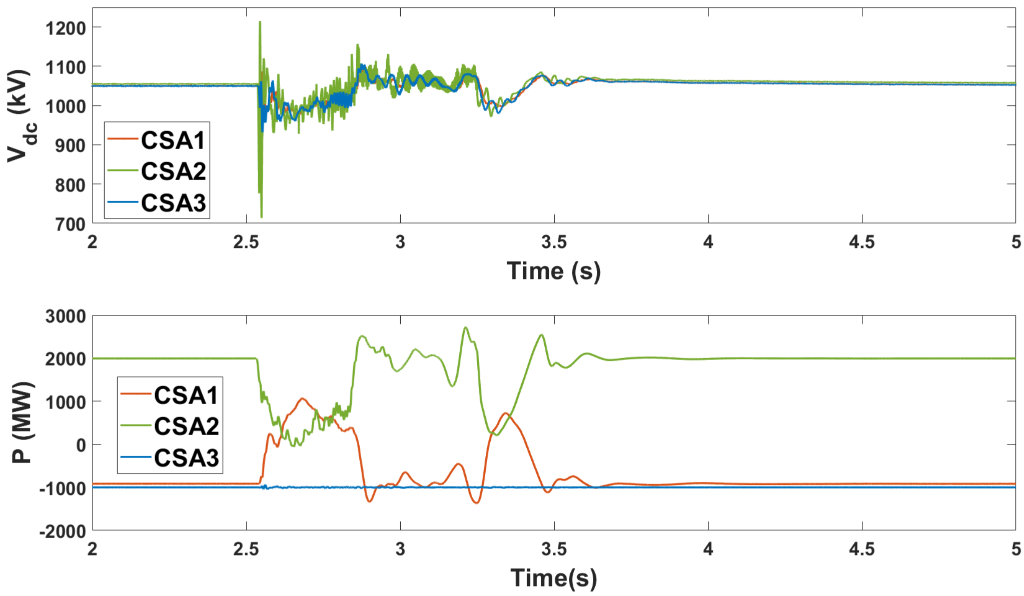

Figure 6.8: DC link voltage and active power plots for different MMCs during L-L fault using PI controller

convergence by the sliding surface to the post-fault operating point. A comparison between the PI and STSMC controller when the system is subjected to L-L-G fault is given in Figure 6.14. As evident, STSMC finds faster settling to the new operating point both for the DC voltage and active power plots, indicating the effectiveness of STSMC controller compared to the state-of-the-art PI controller.

The results from simulation studies demonstrate that the control of negative sequence current components is effective in restoring system stability post fault when compared to the voltage amplitude and phase angle control of GFM converters. The study also indicate that STSMC achieves faster restoration of system stability compared to the conventional PI controller highlighting its superior performance

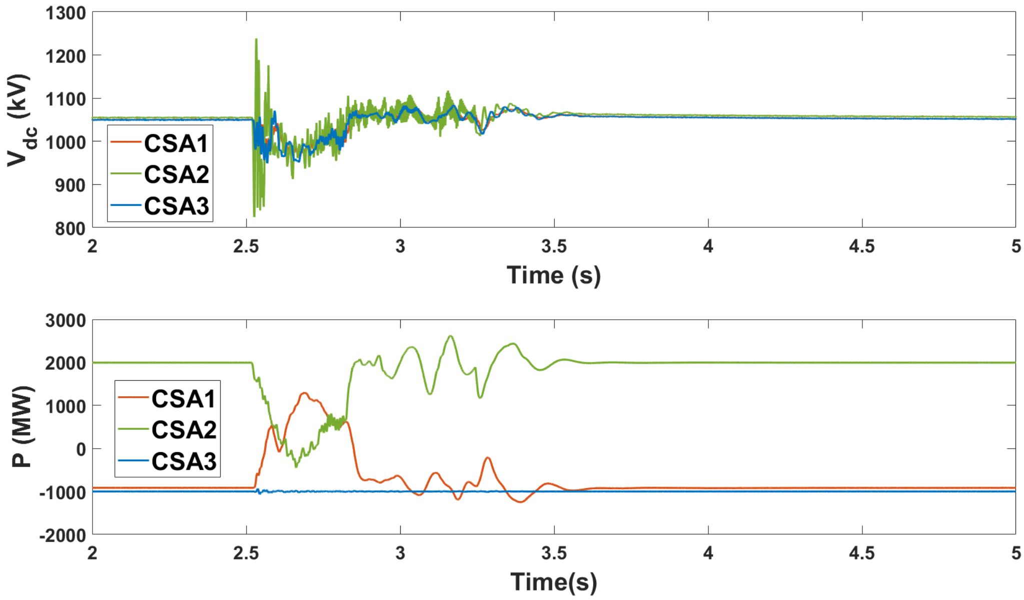

Figure 6.9: DC link voltage and active power plots for different MMCs during L-G fault using PI controller

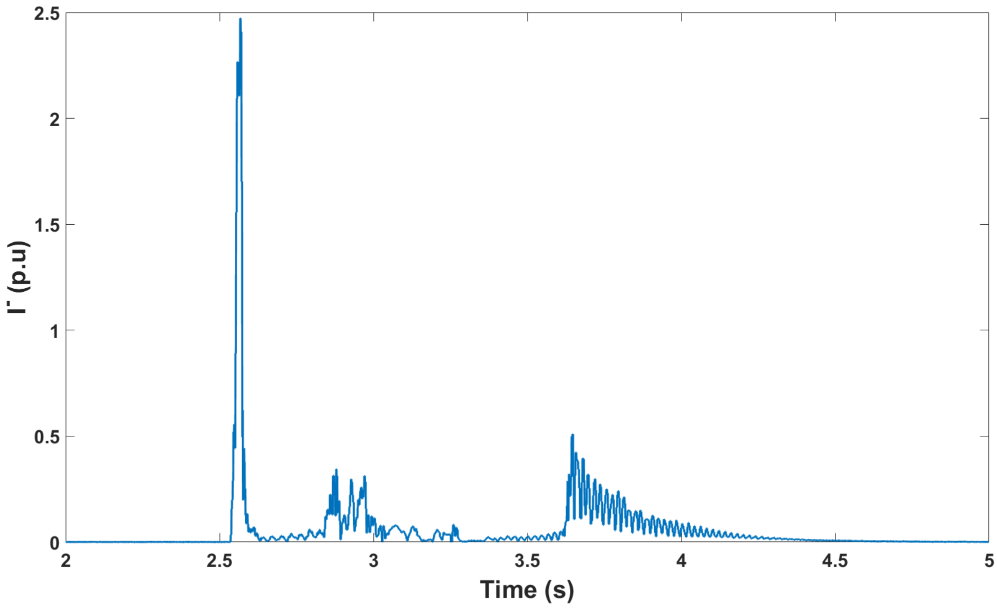

Figure 6.10: Negative sequence current during L-L-G fault using PI controller

in managing dynamic response of power systems.

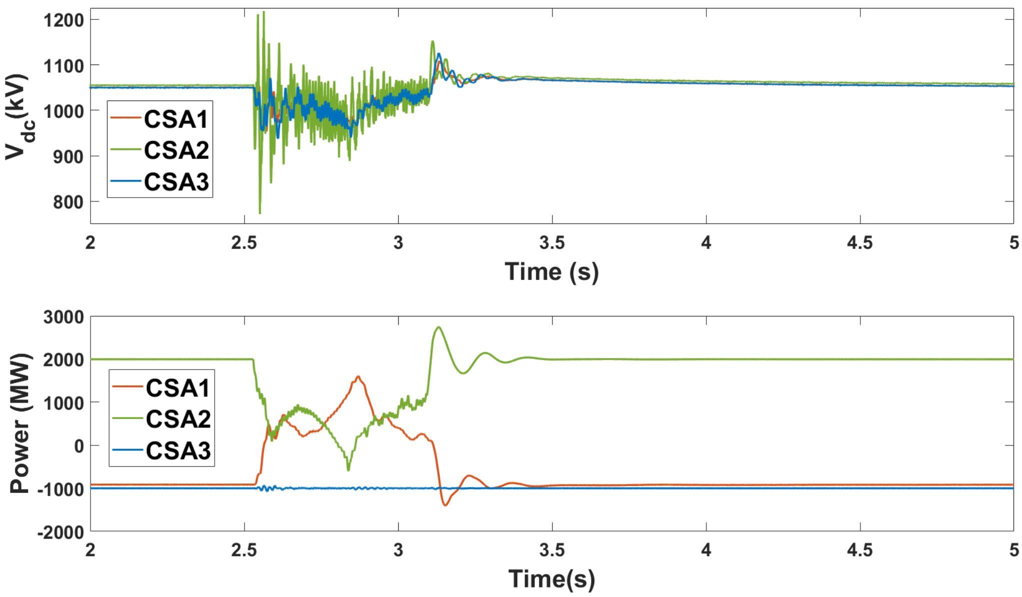

Figure 6.11: DC link voltage and active power plots for different MMCs during L-L-G fault using STSMC

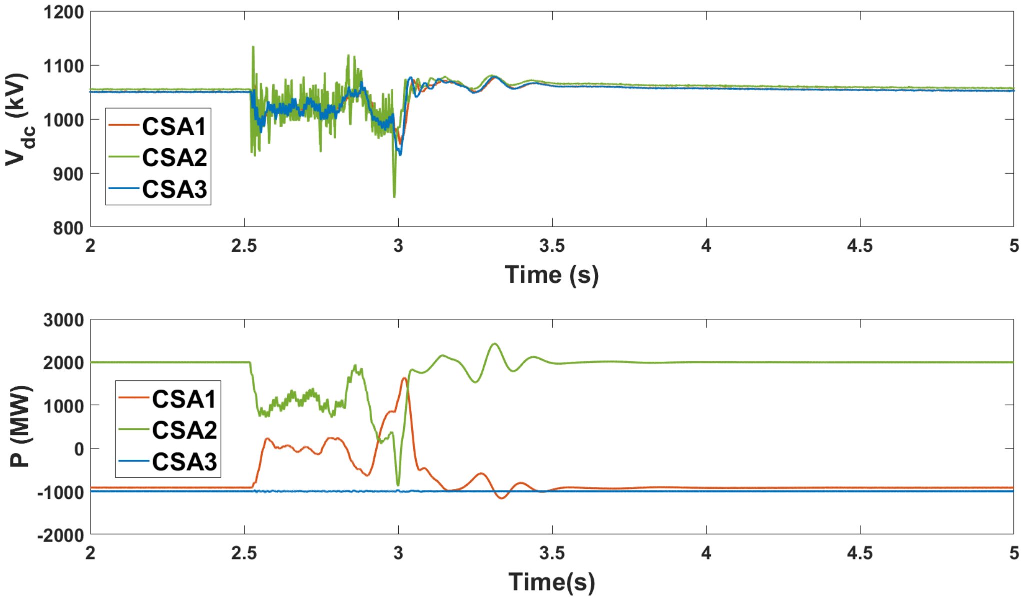

Figure 6.12: DC link voltage and active power plots for different MMCs during L-L fault using STSMC

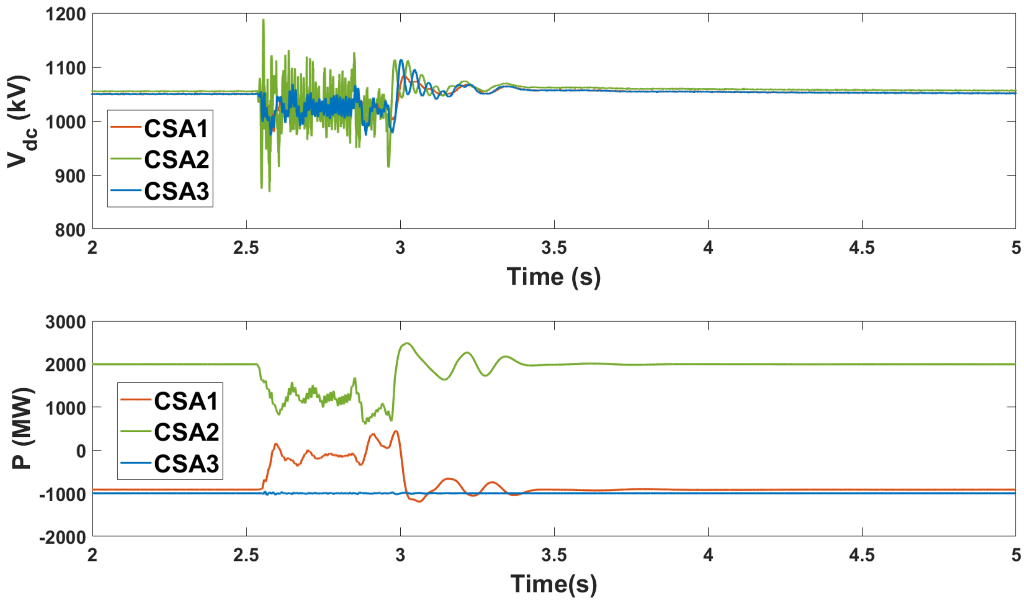

Figure 6.13: DC link voltage and active power plots for different MMCs during L-G fault using STSMC

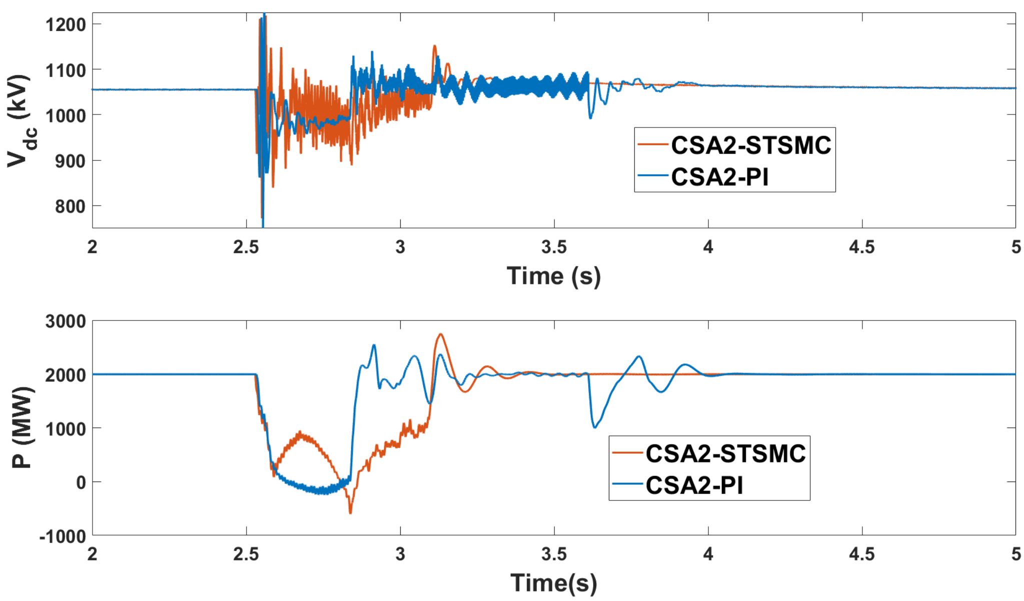

Figure 6.14: DC link voltage and active power plots for CSA2 converter using PI controller and STSMC during L-L-G faults

7
Conclusion & Recommendations

This thesis investigates the fault ride-through capability of MMC-based HVDC systems connected to wind farms, focusing on offshore asymmetrical faults. It addresses four key research questions to understand the behavior of these power systems and ensure effective fault ride-through during offshore asymmetrical faults.

What are the potential issues during an asymmetrical fault?

Asymmetrical faults introduce phase voltage and current imbalances, leading to instability within the power system. These faults are characterized by the generation of substantial negative sequence currents, posing a significant risk of overcurrent conditions that could compromise the integrity of power electronic components. Furthermore, asymmetrical faults can present challenges for protection systems, complicating fault detection and isolation processes. Therefore, comprehensively understanding and effectively mitigating the effects of asymmetrical faults are essential for ensuring the stability of power systems.

What are the characteristics of sequence components during unbalanced fault?

Sequence component analysis is fundamental in fault analysis as it breaks down the system's behavior during faults into positive, negative, and zero sequence components, providing a deeper understanding of fault conditions and their impacts on system stability and protection coordination. During unbalanced faults, power converter-interfaced generation units like wind farms function as controlled current sources in both the positive and negative sequence circuits, unlike conventional generation units, which behave as controlled voltage sources. This distinction leads to differences in fault current behavior between power converter interfaces and systems with synchronous generators. In the event of asymmetrical faults, large negative sequence currents are generated. For grounded faults, zero sequence components are typically present; however, in this study, transformer configurations maintain zero sequence currents close to zero. Consequently, zero sequence voltages are generated during grounded faults. For this study, the large negative sequence current generated serve as a means to detect the presence of the fault. The zero sequence voltage generated during grounded faults aid in differentiation between grounded and non-grounded faults. Additionally, the magnitudes of positive sequence voltages are used to differentiate between line to ground and line to line to ground faults. Overall, analyzing the characteristics of sequence current components during unbalanced faults is crucial for developing effective fault detection, isolation, and mitigation strategies in power systems, ensuring enhanced stability.

How can the sequence current control be utilized to enhance the transient behavior of offshore wind power plants connected to MMC-HVDC systems during unbalanced faults?

Large negative sequence currents are generated during unbalanced faults, causing instability in power systems and resulting in overcurrent that compromises the integrity of power electronic components such as switching valves. Managing sequence currents, particularly negative sequence currents, is crucial in mitigating the adverse effects of asymmetrical faults on system stability. This study adopts the suppression of negative sequence currents in the offshore MMC during fault conditions. It is observed that suppressing negative sequence currents significantly helps to restore power system stability.

How does the dynamic response of the power system improve with the implementation of non-linear control for the MMC converter compared to classical PI control?

Linear and nonlinear controllers are studied to evaluate their effectiveness in the dynamic response of power systems. The Proportional Integral (PI) controller, a linear controller, offers simplicity and robustness. However, due to the nonlinear behavior of MMCs, numerous studies have shown the advantages of nonlinear controllers over PI controllers in enhancing power system performance. In this study, the Super-Twisting Sliding Mode Controller (STSMC) is used for its ease of implementation, fast response, and robustness to uncertainties. Comparing system behavior, it is observed that the STSMC achieves faster settling to the new operating point for both DC voltage and active power signals, demonstrating the STSMC's effectiveness compared to the PI controller.

In conclusion, this study investigates the impact of negative current suppression control during unbalanced offshore AC faults. The control strategy is applied to a three-terminal meshed MMC-HVDC system connecting an offshore wind plant to two onshore AC grids. Various fault scenarios, including line-to-ground, line-to-line, and line-to-line-to-ground faults, are analyzed using this control method. The results demonstrate that controlling sequence current components helps in restoring system stability after fault clearance compared to the voltage amplitude and phase angle control generally used for GFM converters. The study also examines the advantages of using a nonlinear controller, specifically the Super-Twisting Sliding Mode Controller (STSMC) over a linear one. The findings indicate that STSMC achieves faster restoration of system stability compared to the conventional Proportional Integral (PI) controller, highlighting its superior performance in managing the dynamic response of power systems.

7.1. Thesis Contribution

The findings of the thesis have been utilized to enhance the existing RTDS model, specifically focusing on improving its performance under asymmetrical offshore AC faults. This enhancement includes the incorporation of an event-triggered negative sequence current control strategy, aimed at improving the power system stability. As a result, an improved three-terminal meshed MMC-HVDC system model, along with detailed documentation, is now accessible on GitHub. The model also features an algorithm to detect and classify various types of asymmetrical faults by analyzing the characteristics of sequence components.

In addition, a conference paper based on the findings of this research is submitted to the IEEE Power & Energy Society (PES) Innovative Smart Grid Technologies (ISGT) EUROPE, 2024.

7.2. Recommendations

Suppressing negative sequence currents helps to reduce fault currents. However few studies have noted that it can pose challenges for protection systems. Reducing fault currents can result in protection system mal-operation as it may struggle to detect and isolate faults promptly and accurately. Few studies have focused on injecting a controlled negative sequence current which ensures stability as well as enhances the capability of protection system. This is not addressed in the present study as the main focus of this study was to stabilise the power system under asymmetrical fault. Injecting controlled negative sequence currents requires careful consideration of adjustments to the positive sequence currents as well, to manage the over current limitation of the power electronic components. A balanced approach that considers both negative and positive sequence currents and voltages can be investigated for future study that will help to achieve optimal system performance and protection coordination.

Bibliography

[1] Y. Zhang, A. Shotorbani, L. Wang, and W. Li, "Distributed voltage regulation and automatic power sharing in multi-terminal hvdc grids," *IEEE Transactions on Power Systems*, vol. 35, no. 5, 2020.

[2] E. Mehrasa, M.and Pouresmaeil, S. Zabihi, and J. P. S. Catalão, "Dynamic model, control and stability analysis of mmc in hvdc transmission systems.," *IEEE Transactions on Power Delivery*, vol. 32, no. 3, pp. 1471–1482, 2017.

[3] J. Deng, L. Yao, F. Cheng, R. Chen, and X. Li, "An enhanced voltage correction control strategy for asymmetrical fault ride-through of offshore wind power using mmc-hvdc.," *2023 6th International Conference on Energy, Electrical and Power Engineering*, 2023.

[4] T. Roose, A. Lekić, M. M. Alam, and J. Beerten, "Stability analysis of high-frequency interactions between a converter and hvdc grid resonances," *IEEE Transactions on Power Delivery*, vol. 36, no. 6, pp. 3414–3425, 2021.

[5] O. Göksu, N. A. Cutululis, P. Sorensen, and L. Zeni, "Asymmetrical fault analysis at the offshore network of hvdc connected wind power plants," in *2017 IEEE Manchester PowerTech*, pp. 1–5, 2017.

[6] J. Yan, Q. Zeng, Y. Li, and L. Lin, "Research on negative sequnence current coordinated control strategy for severe asymmetric offshore ac faults of wind power transmission system based on mmchvdc," in *2021 Annual Meeting of CSEE Study Committee of HVDC and Power Electronics (HVDC 2021)*, pp. 45–50, 2021.

[7] M. Ndreko, M. Popov, A. A. van der Meer, and M. A. M. M. vdn der Meijden, "The effect of the offshore vsc-hvdc connected wind power plants on the unbalanced faulted behavior of ac transmission systems," *IEEE Int. Energy Conference (ENERGYCON)*, 2016.

[8] L. Shi, G. P. Adam, R. Li, and L. Xu, "Control of offshore mmc during asymmetric offshore ac faults for wind power transmission.," *IEEE Journal of Emerging and Selected Topics in Power Electronics.*, vol. 8, no. 2, pp. 1074–1083, 2020.

[9] H. Ye, W. Chen, H. Wu, W. Cao, G. He, and G. Li, "Enhanced ac fault ride-through control for mmc-integrated system based on active pcc voltage drop.," *Journal of Modern Power Systems and Clean Energy*, 2023.

[10] B. Luo, R. Subroto, C. Wang, and K. Lian, "An improved sliding mode control with integral surface for a modular multilevel power converter," *Energies*, 2022.

[11] L. Liu, A. Shetgaonkar, and A. Lekić, "Interoperability of classical and advanced controllers in mmc based mtdc power system," *International Journal of Electrical Power and Energy Systems*, vol. 148, 2023.

[12] M. Ahmadijokani, M. Mehrasa, M.and Sleiman, M. Sharifzadeh, A. Sheikholeslami, and K. Al-Haddad, "A back-stepping control method for modular multilevel converters.," *IEEE Transactions on Industrial Electronics*, vol. 68, no. 1, pp. 443–453, 2021.

[13] R. Coban, "Backstepping integral sliding mode control of an electromechanical system," *AUTOMATIKA*, vol. 58, no. 3, 2018.

[14] C. W. G. B4.57, “Guide for the development of models for hvdc converters in a hvdc grid,” tech. rep., CIGRE, 2014.

[15] Y. Zhang, A. Shotorbani, L. Wang, and W. Li, “Distributed voltage regulation and automatic power sharing in multi-terminal hvdc grids,” *IEEE TRANSACTIONS ON POWER SYSTEMS*, vol. 35, no. 5, 2020.

[16] W. Jianzhao, *Review of current control stratgies in Modular Multilevel Converter*. PhD thesis, NTNU, 2016.

[17] R. Rosso, X. Wang, M. Liserre, X. Lu, and S. Engelken, “Grid-forming converters: an overview of control approaches and future trends,” in *2020 IEEE Energy Conversion Congress and Exposition (ECCE)*, pp. 4292–4299, 2020.

[18] U. Sing, “Comparative analysis of grid forming and grid following controls for type-3 and type-4wind turbines,” Master’s thesis, Delft University of Technology, 2023.

[19] M. A. Salam, *Symmetrical and Unsymmetrical Faults. In:Fundamentals of Electrical Power Systems Analysis*, pp. 249–316. Springer Singapore, 2020.

[20] C. Wang, Y. Yu, and D. Du, “Improved current differential protection for ac transmission lines of vsc-hvdc system with offshore wind farms,” *2023 2nd International Conference on Power Systems and Electrical Technology (PSET)*, pp. 42–48, 2023.

[21] R. Technologies, “Standardization of renewable energy system modelling,” tech. rep., 2022.

[22] A. Fares, M. H. Nazari, J. Castaneda, and A. Chassiakos, “Two-area system analysis and control using real-time digital simulator,” in *2016 IEEE Green Energy and Systems Conference (IGSEC)*, pp. 1–7, 2016.

[23] A. Shetgaonkar, “Enhanced real-time multi-terminal hvdc power system benchmark models,” tech. rep., TUDelft, 2023.

[24] Z. Gao, “From linear to nonlinear control means: A practical progression,” *ISA Transactions*, vol. 41, no. 2, 2002.

[25] M. Aghahadi, L. Piegari, A. Lekić, and A. Shetgaonkar, “Sliding mode control of the mmc-based power system,” in *IECON 2022 – 48th Annual Conference of the IEEE Industrial Electronics Society*, pp. 1–6, 2022.

[26] Y. Jin, Q. Xiao, Y. Ji, and T. Dragicevic, “A dual-layer back-stepping control method for lyapunov stability in modular multilevel converter based statcom,” *IEEE Transactions on Industrial Electronics*, vol. 69, no. 3, 2022.